DOKUZ EYLÜL UNIVERSITY

GRADUATE SCHOOL OF NATURAL AND APPLIED SCIENCES

BIPED MECHANISM ANALYSIS FOR WALKING ROBOT APPLICATIONS

by

Tolga OLCAY

July, 2010

İZMİR

BIPED MECHANISM ANALYSIS FOR WALKING ROBOT APPLICATIONS

A Thesis Submitted to the
Graduate School of Natural and Applied Sciences of Dokuz Eylül University
In Partial Fulfillment of the Requirements for the Degree of Master of Science
in Mechatronics Engineering

by

Tolga OLCAY

July, 2010

İZMİR

M.Sc THESIS EXAMINATION RESULT FORM

We have read the thesis entitled **"BIPED MECHANISM ANALYSIS FOR WALKING ROBOT APPLICATIONS"** completed by **TOLGA OLCAY** under supervision of **ASST. PROF. DR. AHMET ÖZKURT** and we certify that in our opinion it is fully adequate, in scope and in quality, as a thesis for the degree of Master of Science.

ASST. PROF. DR. AHMET ÖZKURT

Supervisor

(Jury Member)

(Jury Member)

Prof.Dr. Mustafa SABUNCU
Director
Graduate School of Natural and Applied Sciences

ACKNOWLEDGMENTS

I would like to thank to my advisor Asst. Prof. Dr. Ahmet ÖZKURT because of suggestions, helps and supports for the researching and writing of this thesis. I also want to thank to Asst. Prof. Dr. Nalan ÖZKURT and my friend Taner AKKAN because of their encouragements.

Finally, thanks for her helps, patience and love my wife Çiğdem and for all supports my father and mother.

Tolga OLCAY

BIPED MECHANISM ANALYSIS FOR WALKING ROBOT APPLICATIONS

ABSTRACT

This thesis presents a design of biped robots and a cubic spline interpolation based walking trajectory generation method. First for one single step, the foot and hip trajectories is generated by the concept of the cubic spline interpolation. Then it is explained that which design criteria the biped robots ATHO and RUBI have. Also, the joints properties such as joints angles and torques so on are calculated by using inverse and forward kinematic methods. After the simulation of walking trajectories, it is shown the clarification of mechanical structure and actuator specification and experiment results of obtained from walking pattern. While the biped robot is moving, the balance of robot is controlled by the dynamic stability criteria, which is called Zero Moment Point (ZMP).

Keywords: Walking trajectory generation, zero moment points, cubic spline interpolation, biped robot design, stability, actuator specification

YÜRÜYEN ROBOT UYGULAMALARINDA İKİ BACAKLI MEKANİZMA ANALİZİ

ÖZ

Bu tez iki bacaklı robotların tasarımını ve kübik eğri interpolasyonu temelli yürüyüş yörüngesi üretim metodunu sunmaktadır. İlk olarak, tek bir adım için ayak ve kalça yörüngeleri kübik eğri interpolasyonu kavramı ile üretilecektir. Sonra, iki bacaklı robotlar AHTO ve RUBİ'nin hangi tasarım kıstaslarına sahip olduğu açıklanacaktır. Aynı zamanda, eklem açıları ve torkları gibi eklem özellikleri ileri ve ters kinematik metodu ile hesaplanacaktır. Yürüyüş yörüngelerinin simülasyonundan sonra, mekanik yapı ve motorların teknik özelliklerinin açığa çıkarılması ile elde edilen yürüyüş yörüngelerinin deneysel sonuçları gösterilecektir. İki bacaklı robot hareket ederken, robotun dengesi, sıfır moment noktası (SMN) ismi ile bilinen dinamik denge kriterleri ile kontrol edilecektir.

Anahtar sözcükler: Yürüyüş yörüngesi üretimi, sıfır moment noktası, kübik eğri interpolasyonu, iki bacaklı robotların tasarımı, denge, motorlar teknik özellikleri

CONTENTS

Page

CHAPTER ONE
INTRODUCTION

In recent years there has been much interest a walking biped and legged robots (Yamaguchi, Takaniski & Kato, 1993, Tang, Zhou & Sun, 2003). This interest mainly trends biped robots which can operate in human oriented environments. Biped robots have higher mobility than other robots in various environments such as rough terrain, step stair and with obstacles (Huang et al., 2001, Kim & Oh, 2004). Mobility is very important properties of robot for helping and serving humans in all types of environments. It is also much greater efficiency than any other types of robots. Biped robots can be used to difficult or dangerous tasks for human such as working in extreme conditions, with explosive or with toxic material. Other advantages of legged machine, the legs allow the body to move a different trajectory. In other words, the path of upper body may be smooth. Even tough these advantages, the biped robot is not a simple problem. Because, it is unbalanced, nonlinear, dynamically time variant and has a complex control algorithms obstacles (Kim & Oh, 2004).

1.1 History

Man has always been appealing a working machine like the human. Leonardo de Vinci is probably the first man to have drawn a humanoid machine (Figure 1.1).

In the 18^{th} and 19^{th} centuries, some of constructions which reproduced human movement were built. John Brainerd's Steam man and Frank Reade Junior's Electric Man were a sample of these humanoid machines (Chevallereau et al., 2009).

With start of the 20^{th} century, a different type of legged robots construction was started. In the 1980s, people interested in jumping robots at Massachusetts Institute of Technology (Murphy & Raibert, 1985, Raibert & Sutherland, 1983 and Raibert, 1986). Figure 1.2.a and 1.2.b are the samples of MIT's robots.

Figure 1.1 Leonardo de Vinci's Humanoid.

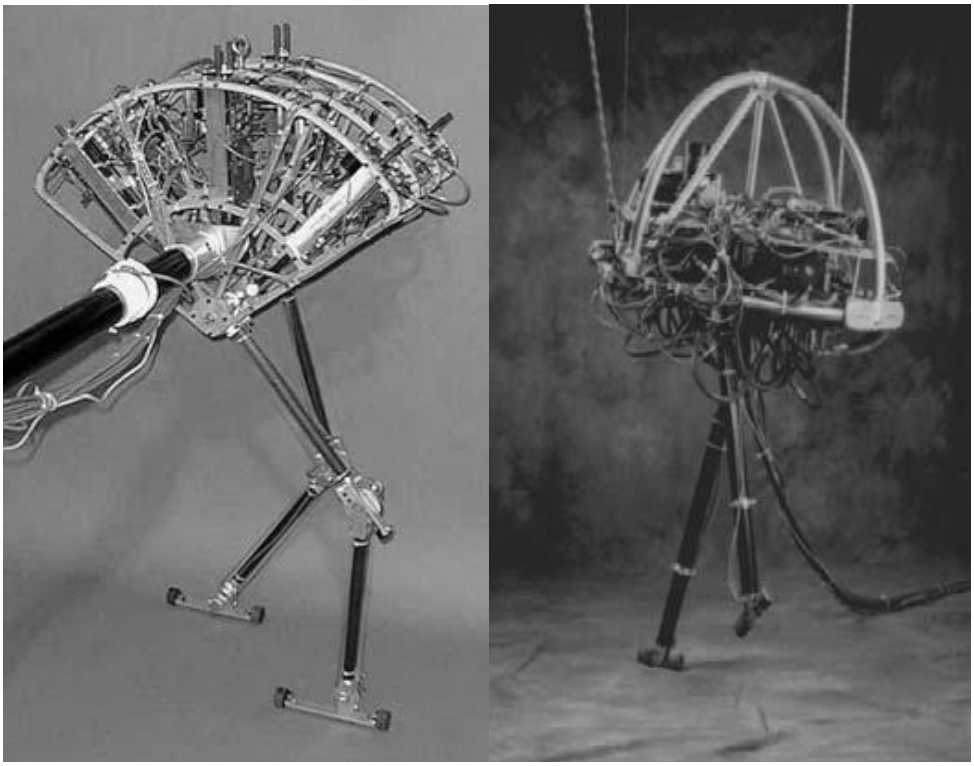

a) Spring Flamingo. b) 3D bipedal robot.

Figure 1.2 MIT laboratory robots.

At the same years, WL-10R was developed in Waseda University, Japan (Figure 1.3.a). Until today, many biped and humanoid robots were built in different countries. While some of these robots had statically stable trajectory (Figure 1.3.b), others had dynamically stable (Figure 1.3.c) (Chevallereau et al., 2009).

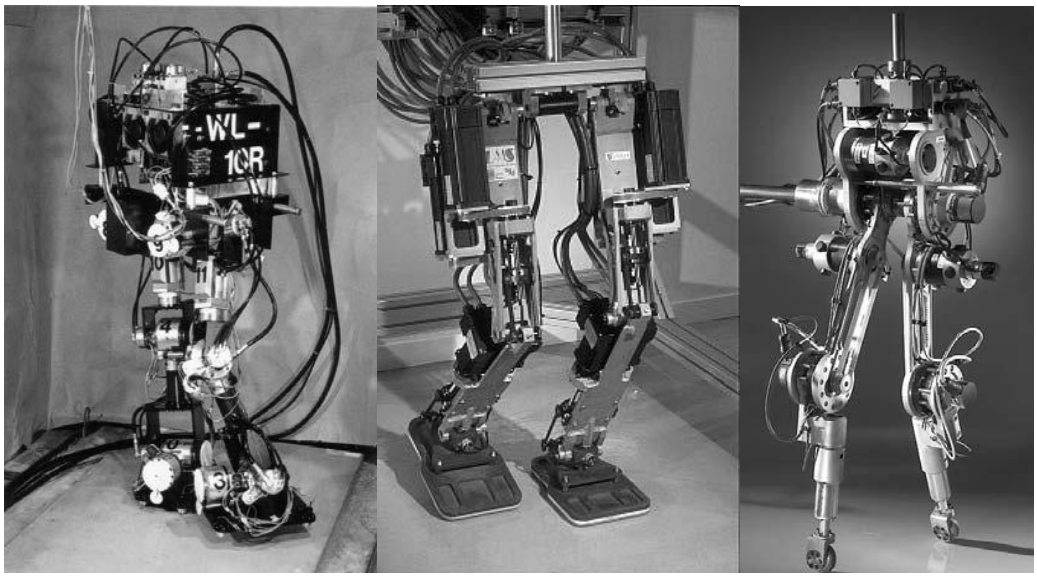

a) WL-10R (Waseda Uni.). b) BIP robot (INRIA). c) Rabbit robot (CNRS).

Figure 1.3 Different types of biped robots.

While it is not yet clear how humans will use biped robots effectively, many companies, research institutes and universities continue to improve knowledge in the subject of biped humanoids robot. The most well known biped humanoid robots in the word are ASIMO of Honda, WABIAN of Waseda University, QRIO of Sony, H-7 of the University of Tokyo and HRP-2 of National Institute of Advanced Industrial Science and Technology. All these reach groups have their own strategies. Each year, they improve their strategies and create new biped robots to reach a more human-like biped robot.

The most often used applications of biped or humanoid robots are service robotics, robotics for dangerous environments, toys and animation robots, defense robotics, medical prostheses and surveillance robots.

1.2 Background

Although humanoid robots are expected to simulate human movement, the human walking is a complex dynamic activity. Because of high degree of freedom (DOF), 3D deformable body structure and complex moving trajectory, the whole human model can not be applied. To over come these problems, many researchers (Nagasaka et al., 1999, Hong, S., 2009 & Huang et al., 2001) have constructed simplified biped robot model.

Structure of biped robot has some constrains such as joint angle range limitation, legs kinematics, joint angle velocity limitation, contact between robot links and so on. However, these constrains are not enough to define the walking trajectory. There are several other criterions to reach the most suitable trajectory. The cost function, the minimum consume energy, the minimum torque change and the global stability are some of them (Tang, Zhou & Sun, 2003, Ha, Han & Hahn, 2007).

The practical technique on walking robot control is consisting of two parts (Hirai et al., 1998). One is the walking pattern generation and other is online stability feedback control.

Stability is a primary requirement of walking trajectory generation for biped robot. There are two type stability, static walking stability and dynamic walking stability. (Tang, Zhou & Sun, 2003)

When the biped robot is in static stability or static balance, the ground of projection of its global center of mass must be in the support foot area. But this case happens when biped robot moves very slowly. So, all moments of links can be neglected. (Tang, Zhou & Sun, 2003)

Different from static stability, dynamic stability or dynamic balance involves the localization of the center of pressure. In other words, it considers dynamic effect of the biped robot. Thus, the global center of mass may lie outside of the support foot

region. But the center of pressure is always within the support foot area. Many studies used to dynamic stability for achieving walking gait (Yamaguchi et al., 1993, Li et al., 1992, Park et al, 1998, Huang et al., 2001 and Tang et al., 2003).

Most popular method of dynamic stability is Zero Moment Point (ZMP). The ZMP is defined as the point on the ground where the total moment of the active forces equal to zero (Vokobratoviç & Borovac, 2004). If the ZMP is within the convex hull of all contact points between the feet and the ground, we can achieve a dynamically stable walking motion.

Another requirement of walking trajectory generation is smooth walking pattern generation. It is curial for a stable motion (Shih, 1997 & Ito, Muakami & Ohnishi, 2002). To achieve smooth walking pattern, all joint trajectories should be continuous at both first and second order derivatives. The first order derivative continuity guarantees the smoothness of velocities. The second order derivative continuity guarantees the smoothness of accelerations. The third order spline interpolation is the most used method to achieve smooth walking trajectories (Huang et al., 2001, Tang et al., 2003 and Thant & Aye, 2009).

Human walking pattern is composed of dynamic motions on the sagittal, frontal and transverse plane. In order to achieve the complete gait of biped robot, gait analyze is done on two or more planes. This work analyses gait pattern on the sagittal and transverse plane. On the sagittal plane, biped robot gait pattern is similar to human gait pattern. The movement of walking mainly takes place in the sagittal plane. All biped robots have the largest number of important articulations in this plane. After finishing gait pattern on the sagittal plane, the pattern on the transverse plane is generated. It is referring the pattern on the frontal plane so that to achieve complete walking pattern and calculate ZMP.

1.3 Research Objectives and Overview

Main goal of this thesis is to develop a biped robot mechanism and its walking sequence. When designing the biped robot, it is aim that human-like leg mechanism and human gait are approached with more suitable energy-performance rate at walking algorithm.

For this purpose, one step of a walking sequence is studied. So that one single step, foot and hip trajectories, joints angles, velocities, accelerations and torques are calculated by using mathematical methods and simulation programs. After that the biped robot mechanism is designed, two different robots are built and made experiment in view of the fact that obtained results. The obtained data become implementable to joints actuators and robots. Designed biped robots are shown in Figure1.1, Chapter Three and Appendix A.

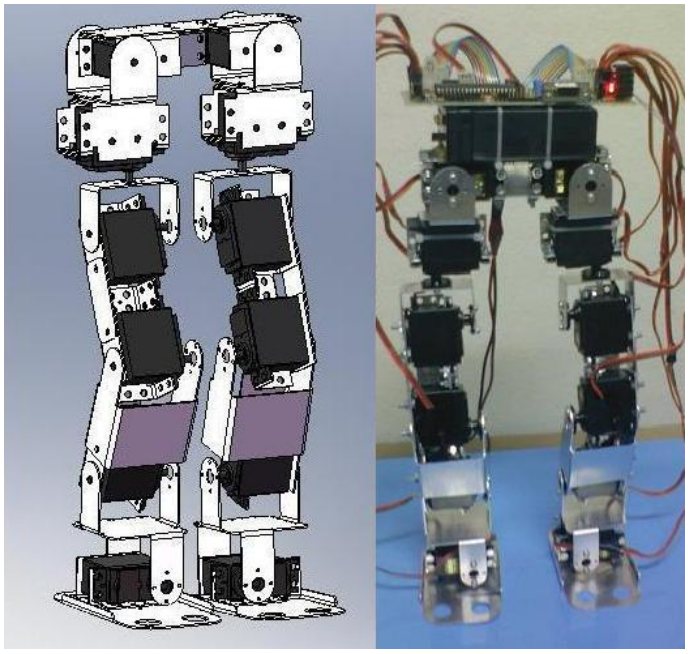

a) First biped robot model, AHTO.

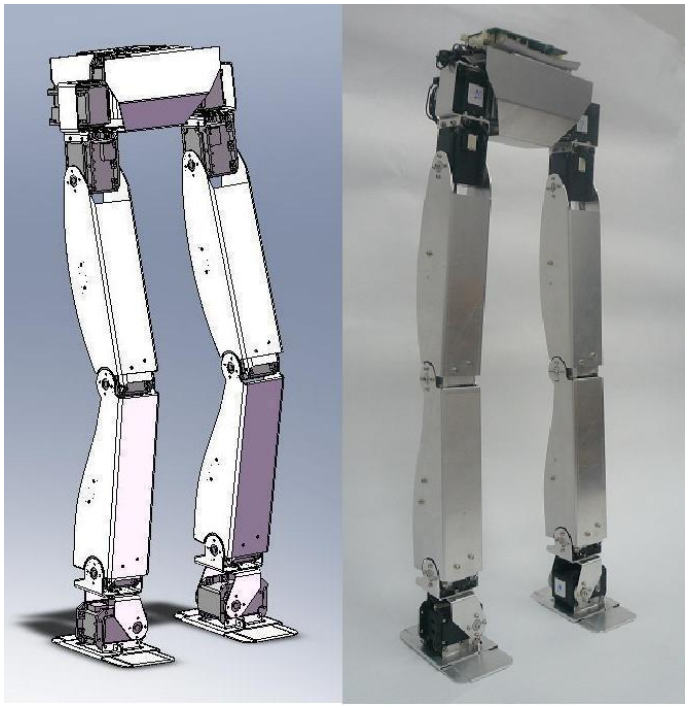

b) Second biped robot model, RUBI.

Figure 1.1 Designs of biped robot models

Due to the feedback from biped robot joints can not be acquired from first designed robot, the balance of robot provides from feedback of accelerometer in robots trunk. In this case, despite of position of each joint moving, total moving of biped robot can be analyzed.

To reach realistic joint movements, it is essential to get feedback from joint simultaneously. Therefore, second robot is built and used appropriate actuators. With these actuators, joints or actuators position, velocity, torque, temperature feedbacks are obtained in real time. Thus, more powerful biped robot and more stable walking control algorithm can be evaluated.

Parallel with this study, walking robot control circuit and motion experiments are being continued by other teams which are responsible for final motion. In this thesis, only mechanical designs and one single step walking sequence of robots are investigated.

This thesis is organized as follows. Chapter two explains the walking cycle analyses. Chapter three presents the design of the biped robots. Chapter four presents the execution of walking pattern of biped robot and experiments of gait generations. In chapter five, conclusion and future work are given finally.

CHAPTER TWO
WALKING CYCLE ANALYSIS

Biped walking is a periodic phenomenon. A complete humanoid robot walking cycle is divided into two phase: a single-support phase and a double-support phase (Ha, Han & Hahn, 2007). In the single-support phase, while one foot is stationary on the ground, the other foot is moving from back backward to forward. In the double-support phase, both humanoid robot feet are in contact with the ground. The double-support phase begins with the heel of the forward foot touching the ground, and ends with the toe of the rear foot leaving the ground. The single-support phase begins with the toe of the rear foot leaving the ground, and ends with the heel of the forward foot touching the ground.

If a double-support phase is instantaneous or too short, the hip of robot has to move fast. So the robot's center of gravity or ZMP must be transferred from the rear foot to the front foot in a short time. That affects robot's stability badly. On the other hand, if the interval of double-support phase is too long, it is difficult for the robot to walk at high speed (Huang et al., 2001). The interval of double-support phase in human motion is about %20 (McMahon, T. A., 1984, Inman, V.T., 1981).

In order to achieve the walking cycle of biped robot like human, the cycle is analyzed on the sagittal, frontal and transverse plane. Since the simplified structure of biped robot, this thesis analyzed dynamic elements on the sagittal and transverse plane.

On the frontal plane, it is assumed that the biped robot's legs are always parallel. Also it is assumed that the biped robot's feet are parallel with ground. Thus the angels of four joint have same value as shown in Figure 2.1.

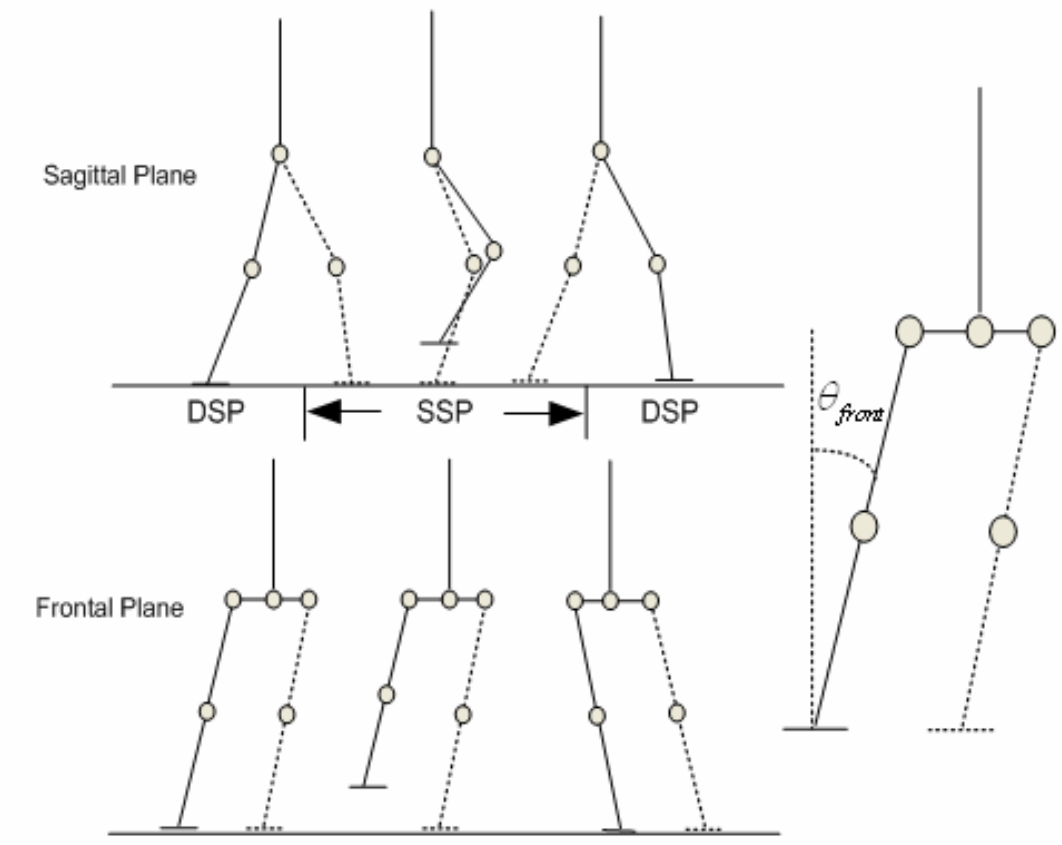

Figure 2.1 Walking patterns on the sagittal and frontal plane.

The walking pattern can be denoted with knowing both foot trajectories and hip trajectories. If they are known, all joint angles of the biped robot will be determined by using forward kinematics.

On the sagittal plane, Huang et al., (2001) expressed foot trajectories by a vector $X_a = [x_a\ t\ , z_a\ t\ , \theta_a\ t\ ]^{\mathrm{T}}$, where $(x_a\ t\ , z_a\ t\ )$ is the coordinate of the ankle position, and $\theta_a\ t$ is the angle of the foot. Also hip trajectory was expressed by a vector $X_h = [x_h\ t\ , z_h\ t\ , \theta_h\ t\ ]^{\mathrm{T}}$, where $(x_h\ t\ , z_h\ t\ )$ is the coordinate of the hip position, and $\theta_h\ t$ is the angle of the hip (Figure 2.2).

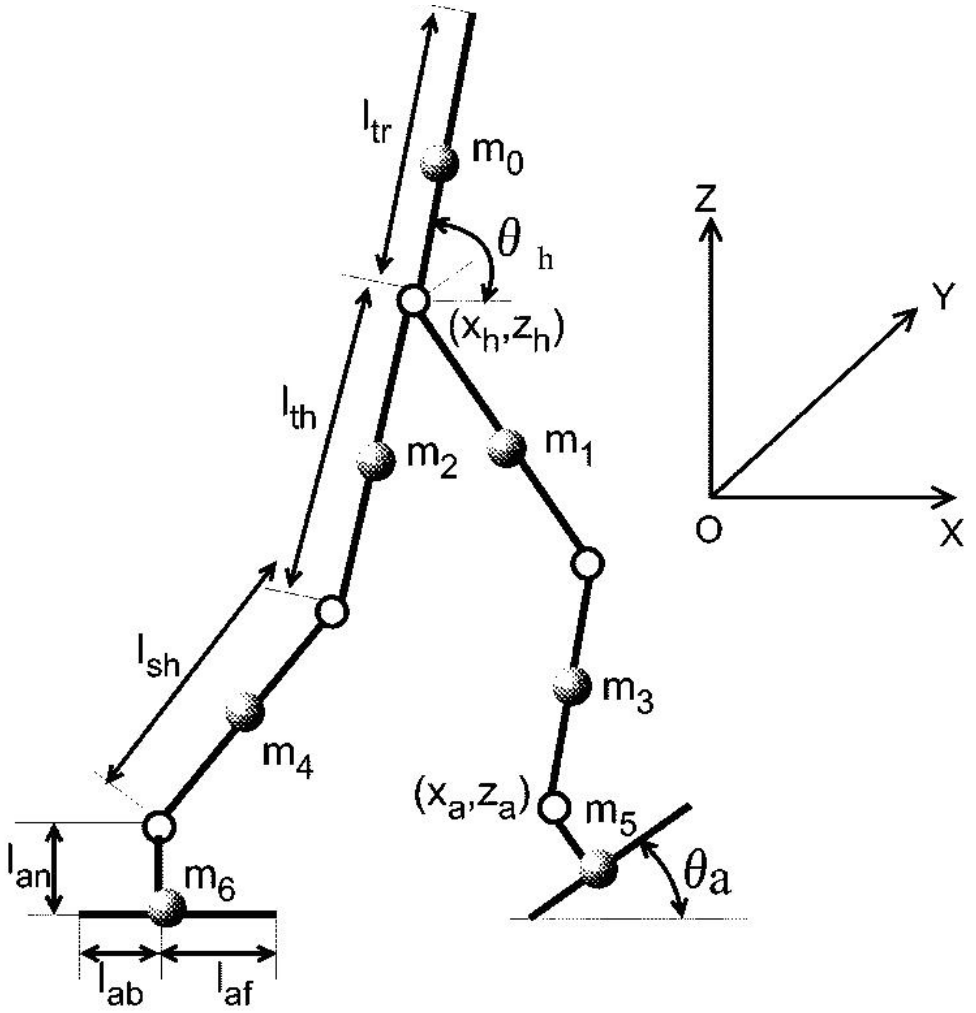

Figure 2.2 Walking biped robot.

2.1 Foot Trajectories

This thesis is only interested in the generation of the left foot trajectory. The right foot trajectory is same as the left foot trajectory except for a delay. To calculate robot trajectories is necessary that making some assumption and description about robot parameters (Huang et al., 2001).

The period for one walking step is T_c. The k'th walking step begins when the heel of the left foot leaving the ground at $t = kT_c$ and ends when the heel of the left foot contacting the ground at $t = k+1\ T_c$. Where k = 1, 2, 3…,K, K is the number of step.

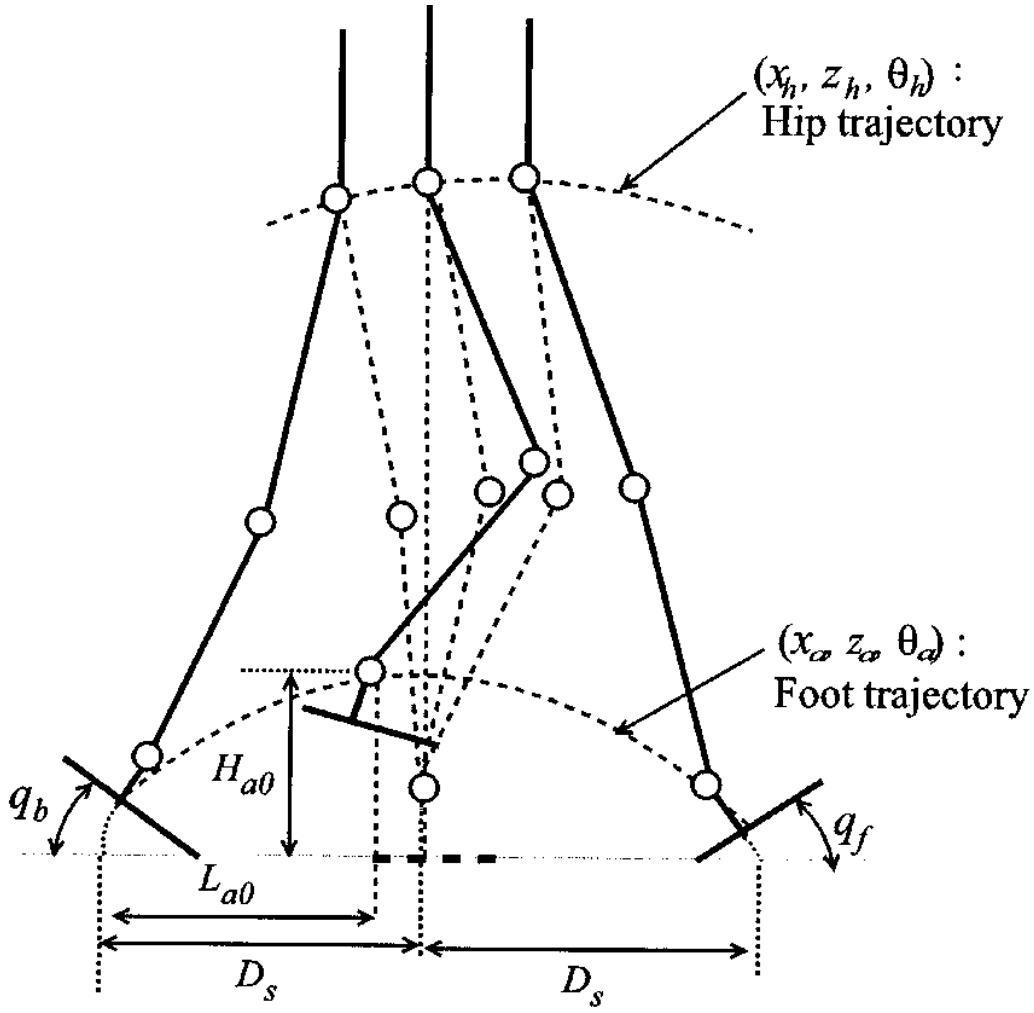

Figure 2.3 Walking parameters of humanoid biped robot.

The angle of foot as it leaves on the ground is q_b, the angle of foot as it lands on the ground is q_f as shown in Figure 2.3. T_d is the interval of the double-support phase. Assuming that the sole of the right foot is in contact with the ground following constrains are obtained for $\theta_a \ t$:

$$\theta_a \ t = \begin{cases} q_{gs}(k), & t = kT_c \\ q_b, & t = kT_c + T_d \\ -q_f, & t = \ k+1 \ T_c \\ -q_{ge}(k), & t = \ k+1 \ T_c + T_d \end{cases} \tag{1}$$

where $q_{gs}(k)$ and $q_{ge}(k)$ are the angels of the ground surface which under the support foot (the right foot in this case). $q_{gs}(k) = q_{ge}(k) = 0$, if the support foot is on level ground.

L_{ao} and H_{ao} are the position of the highest point of the swing foot ankle that is important if there are obstacles in environments and T_m is the time that the swing foot reaches the highest position. D_s is the length of one step (Figure 2.3), l_{an} is the height of the foot, l_{ab} is the length from the ankle joint to the heel, l_{af} is the length from the ankle joint to the toe (Figure 2.2).

Thus, above constrains are obtained for $x_a\ t$:

$$x_a\ t = \begin{cases} kD_s, & t = kT_c \\ kD_s + l_{an}\sin q_b + l_{af}(1-\cos q_b), & t = kT_c + T_d \\ kD_s + L_{ao}, & t = kT_c + T_m \\ (k+2)D_s - l_{an}\sin q_f - l_{ab}(1-\cos q_f), & t = (k+1)T_c \\ (k+2)D_s, & t = (k+1)T_c + T_d \end{cases} \quad (2)$$

and for $z_a\ t$:

$$z_a\ t = \begin{cases} h_{gs}(k) + l_{an}, & t = kT_c \\ h_{gs}(k) + l_{af}\sin q_b + l_{an}\cos q_b, & t = kT_c + T_d \\ H_{ao}, & t = kT_c + T_m \\ h_{ge}(k) + l_{ab}\sin q_f + l_{an}\cos q_f, & t = (k+1)T_c \\ h_{ge}(k) + l_{an}, & t = (k+1)T_c + T_d \end{cases} \quad (3)$$

where $h_{gs}(k)$ and $h_{ge}(k)$ are the heights of the ground surface which under the support foot (the right foot in this case). $h_{gs}(k) = h_{ge}(k) = 0$, if the support foot is on level ground.

To obtain a smooth trajectory,

1. The first derivatives terms $\dot{x}_a\ t\ ,\dot{z}_a\ t$ and $\dot{\theta}_a\ t$ be zero at $t = kT_c$ and $t = \ k+1\ T_c + T_d$,

2. The first derivatives terms $\dot{x}_a\ t\ ,\dot{z}_a\ t$ and $\dot{\theta}_a\ t$ be differential,

3. The second derivatives terms $\ddot{x}_a\ t\ ,\ddot{z}_a\ t$ and $\ddot{\theta}_a\ t$ be continuous at all breakpoints t.

Using polynomial interpolation is difficult for computation and the polynomial will be too high to satisfy above conditions. But there is a usage of third-order interpolation, the second derivatives $\ddot{x}_a\ t\ ,\ddot{z}_a\ t$ and $\ddot{\theta}_a\ t$ are always continuous. Therefore, using third-order interpolation is best way to find $x_h\ t\ ,z_h\ t$ and $\theta_h\ t$.

2.2 Hip Trajectories

If there is no upper body, the angle of the hip $\theta_h\ t$ will be selected constant. When determining the hip motion, the important point is the ZMP. The change of $z_h\ t$ hardly affects the calculation of the ZPM. So we can determine $z_h\ t$ to be constant or within a fixed range. If $z_h\ t$ is within a fixed range, above constrains are obtained:

$$z_h\ t\ = \begin{cases} H_{h\min}, & t = kT_c + 0.5T_d \\ H_{h\max}, & t = kT_c + 0.5(T_c - T_d) \\ H_{h\min}, & t = \ k+1\ T_c + 0.5T_d \end{cases} \qquad (4)$$

where $H_{h\min}$ is the lowest position of the hip at the middle of the double-support phase and $H_{h\max}$ is the highest position of the hip at the middle of the single-support phase.

On the other hand, the change of $x_h \ t$ directly affects the ZPM and the stability of a biped robot. Dasgupda & Nakamura (1999), Tang, et al. (2007), Ha, Han & Hahn (2007) have presented methods for finding the hip trajectory. Some methods are not enough to desire ZMP trajectories. Huang et al., (2001) propose the following method to reach desired ZMP trajectories. There is important parameter are x_{sd} that is distance from the hip to the ankle of the support foot at the start of the single-support phase and x_{ed} that is distance from the hip to the ankle of the support foot at the end of the single-support phase on the sagittal plane (Figure 2.4). Thus, above constrains are obtained for $x_h \ t$:

$$x_h \ t \ = \begin{cases} kD_s + x_{ed}, & t = kT_c \\ (k+1)D_s - x_{sd}, & t = kT_c + T_d \\ (k+1)D_s + x_{ed}, & t = (k+1)T_c \end{cases} \tag{5}$$

To satisfy first and second derivatives constrains, third-order interpolation is used. Also x_{sd} and x_{ed} be vary within a fixed range (Huang et al., 2001).

$$\begin{cases} 0,0 < x_{sd} < 0,5D_s \\ 0,0 < x_{ed} < 0,5D_s \end{cases} \tag{6}$$

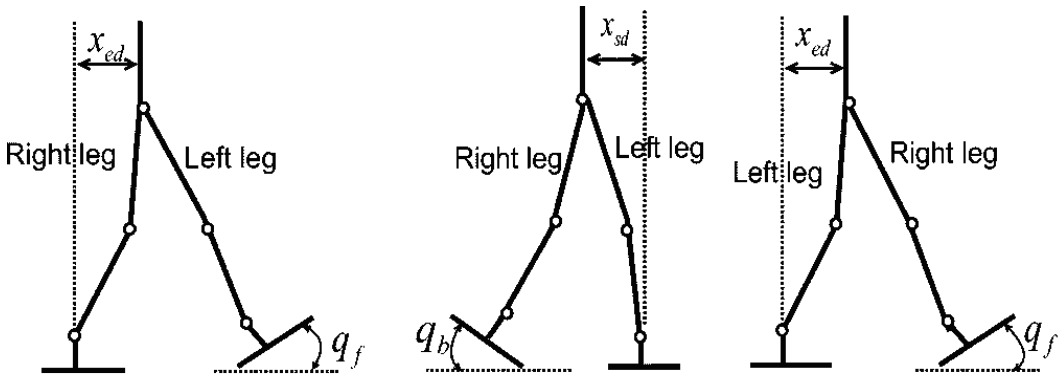

Figure 2.4 Hip position of the biped robot in the walking cycle.

2.3 Zero Moment Point Criterion

The zero moment point (ZPM) is defined as the point on the ground about which the sum of all the moments of the active forces equal zero. The ZPM can be calculated using the following equations (Vokobratoviç & Borovac, 2004):

$$x_{zmp} = \frac{\sum_{i=1}^{n} m_i(\ddot{z}_i + g)x_i - \sum_{i=1}^{n} m_i \ddot{x}_i z_i - \sum_{i=1}^{n} I_{iy}\ddot{\Omega}_{iy}}{\sum_{i=1}^{n} m_i(\ddot{z}_i + g)} \tag{7}$$

$$y_{zmp} = \frac{\sum_{i=1}^{n} m_i(\ddot{z}_i + g)y_i - \sum_{i=1}^{n} m_i \ddot{y}_i z_i - \sum_{i=1}^{n} I_{ix}\ddot{\Omega}_{ix}}{\sum_{i=1}^{n} m_i(\ddot{z}_i + g)} \tag{8}$$

where m_i is the mass of link i, (x_i, y_i, z_i) is the coordinate of the mass center of link i, $(\ddot{x}_i, \ddot{y}_i, \ddot{z}_i)$ is the accelerations of the mass center of link i, I_{ix} and I_{iy} are the inertial components, $\ddot{\Omega}_{ix}$ and $\ddot{\Omega}_{iy}$ are the absolute angular velocity component around x–axis and y-axis at the center of gravity of link i, g is the gravitational acceleration, $(x_{zpm}, y_{zpm}, 0)$ is the coordinate of the ZPM on an absolute Cartesian coordinate system.

The ZPM determines the biped robot's stability. If the ZPM is located in supported foot area, the biped robot is able to walk. Otherwise the robot tips over. The minimum distance (d_{zpm}) between the ZMP and the boundary of the stable region (supported foot area) is called the stability margin (Figure 2.5).

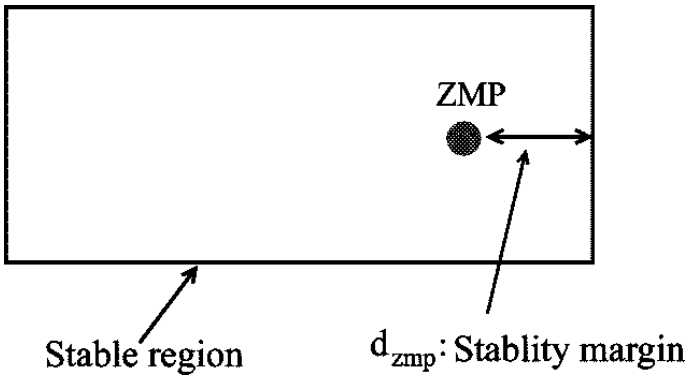

Figure 2.5 Stable region and stability margin.

Using the equations (7) and (8), the ZPM of the biped robot can be designed on the transverse plane as shown in figure 2.6.

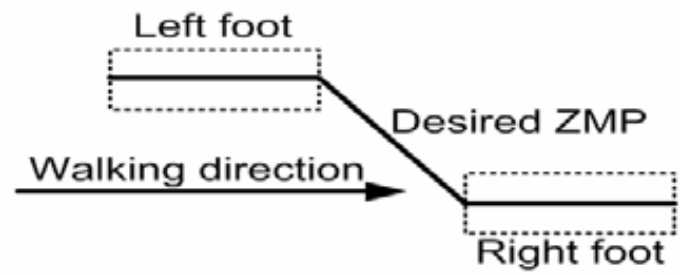

Figure 2.6 Desired ZPM.

CHAPTER THREE
DESING OF THE BIPED ROBOT

When creating a walking biped robot, there are many criteria's to take into consideration: mechanical design, actuator type, sensors, production cost, et al. Thus, robot model designer has to make difficult compromises (Chevallereau et al., 2009).

The many of models presented in introduction chapter are based on the kinematics of the legs only. Therefore, the locomotion system of bipedal robot is limited to 12 degrees of freedom (DOF).

In this thesis, two different biped robot models were produced. First one is named AHTO that was built at the beginning of the work period (Figure 3.1). It is based on Vigor VS-2 servos. All walking pattern generation, simulation and analysis were applied on it.

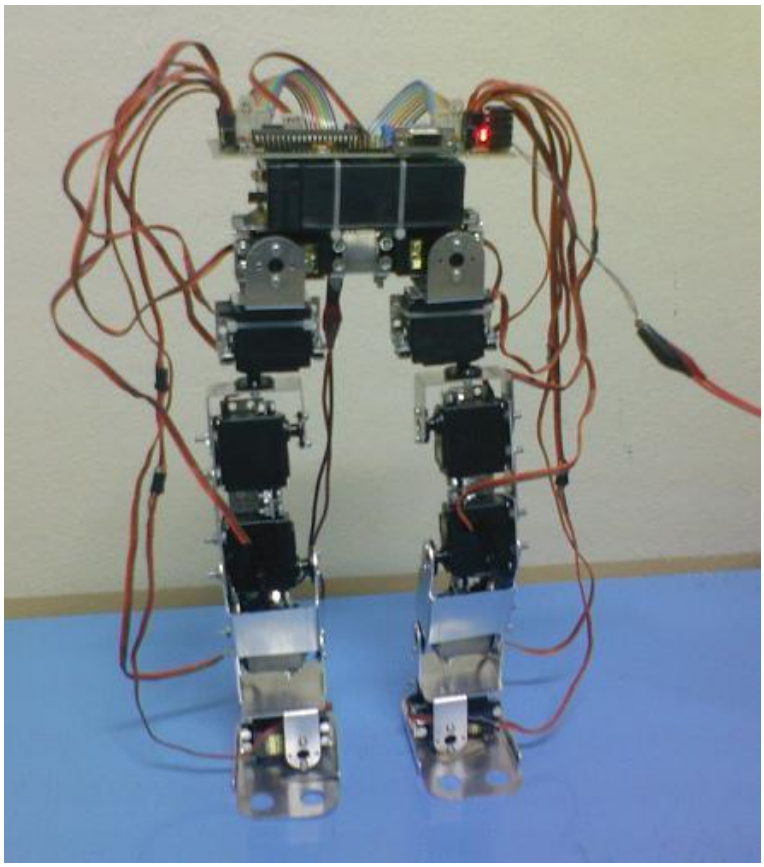

Figure 3.1 First biped robot model, AHTO.

According to the practice result and the referring of the mechanical and physical problems, second biped robot model that is named RUBI was built (Figure 3.2).

Figure 3.2 Second biped robot model, RUBI.

3.1 Mechanical Design

When making mechanical design, many theoretical studies and simulations are needed to harmonize the desired criteria of existing solutions.

AHTO and RUBI were developed according to following design philosophy,

- Human like shape with a trunk.
- Human like movements.
- Compact size and lightweight.
- Kinematically simple structure.
- Low power required.

Each model has a trunk and two legs and each leg consists of a thigh, a shin and a foot (Figure 3.1 & Figure 3.2).

The degrees of freedom of the robots are summarized in Table 3.1.

Table 3.1 Degrees of freedom of AHTO and AHTO-1.

Joint	**Direction**	**Degrees of freedom**
Hip	x, y, z	3 d.o.f x 2 = 6 d.o.f.
Knee	y	1 d.o.f x 2 = 2 d.o.f.
Ankle	x.y	2 d.o.f x 2 = 4 d.o.f.
		12 d.o.f.

3.1.1 AHTO

Biped robot AHTO was designed with SolidWorks which is 3D CAD design software. When designing AHTO, main design factor was servo motors assembly. Thus, it is consist of 42 parts. After the design process, the parts of robot were prepared by laser cutting. SolidWorks model of the biped robot AHTO and its joints structure is shown in Figure 3.3

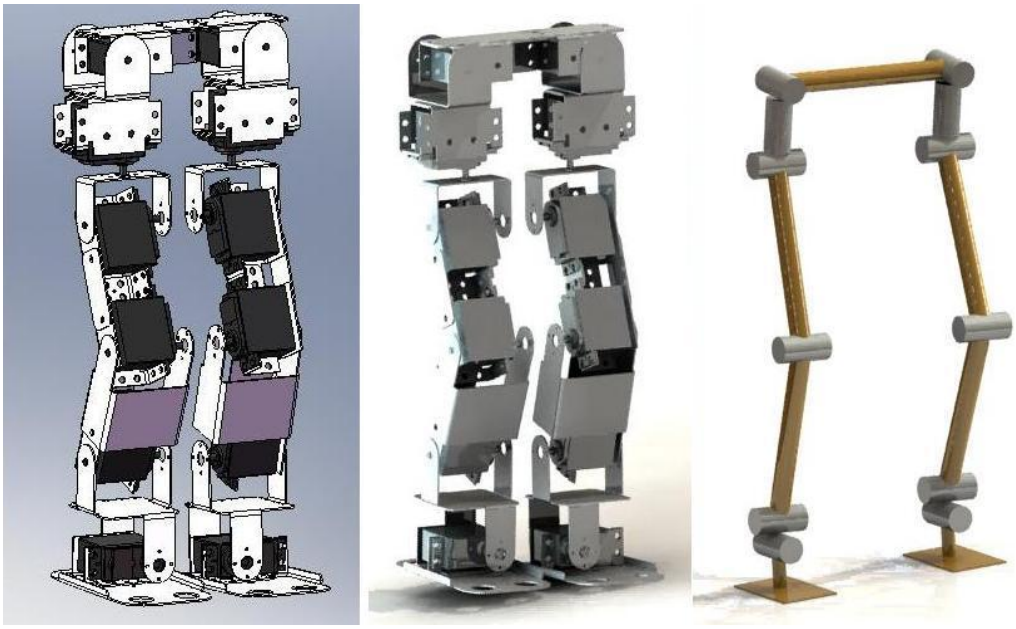

Figure 3.3 SolidWorks model of the biped robot AHTO and its joints structure.

The height, weight and total degrees of freedom of AHTO are 342 mm, 0,51 kg and 12 d.o.f. AHTO is actuated by Vigor VS-2 servos. Detailed technical drawings of AHTO are seen in Appendix A. The dimensions of AHTO are shown in Table 3.2.

Table 3.2 Dimensions of AHTO.

Height	342 mm
Width	150 mm
Depth	52 mm
Length of a thigh (the hip to the knee)	77 mm
Length of a shin (the knee to the ankle)	75 mm
Length of a ankle (the ankle to the foot)	75 mm

3.1.2 RUBI

Like AHTO, biped robot RUBI was designed with SolidWorks. It was designed resemble a child-sized human. Human-robot dimension ratio is approximately 2.3. It is consist of 36 parts. Also, the parts of RUBI were prepared by laser cutting. SolidWorks model of the biped robot RUBI and its joints structure is shown in Figure 3.4.

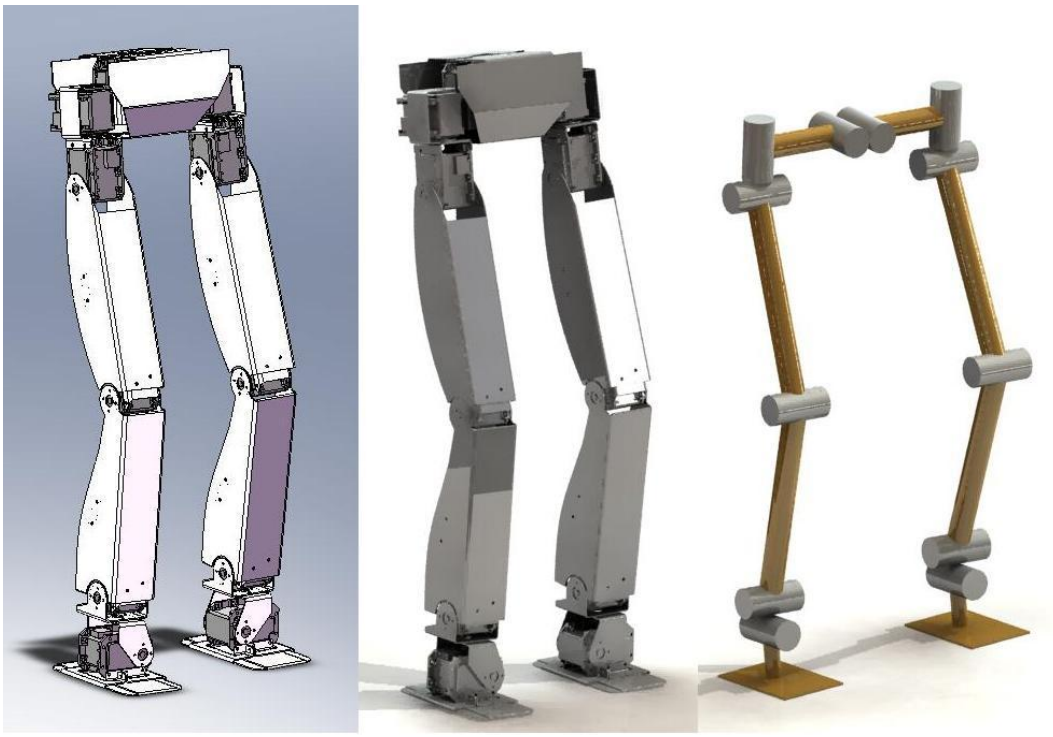

Figure 3.4 SolidWorks model of the biped robot RUBI and its joints structure.

The height, weight and total degrees of freedom of RUBI are 507 mm, 1,24 kg and 12 d.o.f. RUBI is actuated by Dynamixel RX-28 servos. Detailed technical drawings of AHTO are seen in Appendix B. The dimensions of RUBI are shown in Table 3.3.

Table 3.3 Dimensions of RUBI.

Height	507 mm
Width	175 mm
Depth	72 mm
Length of a thigh (the hip to the knee)	177 mm
Length of a shin (the knee to the ankle)	167 mm
Length of a ankle (the ankle to the foot)	68 mm

3.2 Actuators

Walking machines need actuators for leg movement. Usually the actuators provide a torque to move a joint. A single joint of a human cannot move more than

an angle of 300^0. Thus, generally servo motors are used. A servo can provide high torques with having a small size. Also it has the high positioning accuracy.

3.2.1 Vigor VS-2 Servos

Vigor VS-2 Actuators are standard actuators controlled by analog communication. It has plastic gears and generally used for Radio controlled aircrafts (Figure 3.5).

Figure 3.5 Vigor VS-2 servo.

The Specifications of Vigor VS-2 servos are shown in Table 3.4.

Table 3.4 The Specifications of Vigor VS-2 servos.(www.servodatabase.com/servo/vigor/vs-2,2010)

Torque	3.2 kg.cm @ 4.8 V (3.5 kg.cm @ 6V)
Speed	0.2 sec./60 degrees @ 4.8 V(0.17 sec./60 degrees @ 6 V)
Length	40.6 mm
Breadth	20 mm
Height	38.9 mm
Weight	37 grams
Operating Angle	360 degrees
Operating Voltage	4.8-6 V

3.2.2 Dynamixel RX-28 Servos

Dynamixel RX-28 Robot Actuators that are used at RUBI, are high-performance actuators controlled by digital packet communication (Figure 3.6). They include all the functionality a robot enthusiast may require for controlling joints. Their integrated controller allows these servo actuators to be daisy chained for simple control of complex assemblies.

Figure 3.6 Dynamixel RX-28 servo.

Dynamixel RX-28 Robot Actuator features (http://www.robotshop.ca/robotis-cx-28-serial-servo-3.html, 2010):

- Networked communication: Dynamixels can be daisy-chained and communicate at up to 1Mbps. Dynamixels that have a unique ID are controlled by packet communication on a bus (Figure 3.7).
- Precise position control: Offer an excellent resolution of 1024 divisions.
- Powerful feedback: It can provide current position or speed as well as information regarding internal temperature, supply voltage and target position.

- Alarm function: When internal temperature, torque or supply voltage exceeds defined range, it provides feedback about that situation and can automatically correct the situation.

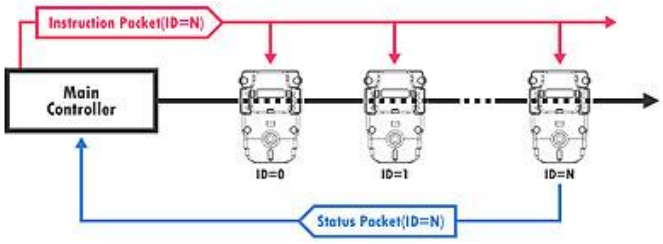

Figure 3.7 Dynamixel RX-28 communications.

- Compliance Driving: Control the amount of elastic force in position control.
- Torque set up: Torque can be set up by 1023 steps from maximum torque to free run state.
- Low current consumption/high voltage operation: Its efficiency is high because it runs at a higher voltage and improves the performance of your robotic system due to its low current consumption.
- Status LED: It has an LED that serves to provide visual feedback on the state of the Dynamixel.

The Specifications of Dynamixel RX-28 servos are shown in Table 3.5.

Table 3.5 The Specifications of Dynamixel RX-28 servos.

Torque	28.3 kg.cm @ 12 V (37.7 kg.cm @ 16V)
Speed	0.167 sec./60 degrees @ 12 V(0.126 sec./60 degrees @ 16 V)
Length	50.6 mm
Breadth	35.6 mm
Height	35.5 mm
Weight	72 grams
Operating Angle	360 degrees
Operating Voltage	11-16 V
Gear Ration	1:193

3.3 Control Units

3.3.1 Parallax Servo Controller

The Parallax Servo Controller (Figure 3.8) controls up to 16 servos, and may be networked together so that two PSC's can control 32 servos using a single USB port to I/O line. The PSC manages all of the servo pulses which enable your microcontroller to take care of more important aspects of the application.

Figure 3.8 Parallax Servo Controller.

To make the application development process easier, a free graphical user interface can be used to make a direct link between mouse and servo movement. Move the mouse, the servo moves in real-time.

Parallax Servo Controller features:
(http://www.parallax.com/Store/Accessories/MotorServoControllers/tabid/160/ProductID/376/, 2010)

- Runtime Selectable Baud rate - A serial message switches the baud rate from: 2400 to 38k4 Baud.
- Controls 16 Servos - All servos driven simultaneously all of the time. 180 degrees of rotation.
- Servo Ramping - 63 ramp rates (0.75 - 60 seconds) allow the user to set the speed of each servo on a per-move basis. There may be chosen one of 63 ramp rates for each servo. The ramping function allows you to individually set the speed of each servo. With ramping, that can tell the servo where to go, and just how fast to get there. The result is true, "set-it and forget-it" functionality. Speed range for 0 - 180 degrees of rotation is 3/4 of a second to 60 seconds.
- Position Reporting - User may request position of an individual servo at any time. This command allows you to request the position of a servo channel, be it stationary or on the move.
- Network Ready - Two modules may be linked together to drive 32 servos at the same time. It is possible to network 2 Parallax Servo Controllers together to control up to 32 servos. Simply use a second 3-Conductor cable to daisy chain two PSCs together as shown in the documentation. The presence of a shunt differentiates between Unit 0 (channels 0-15) and Unit 1 (channels 16-31).
- Enhanced Resolution - Use of 16-bit PWM timers enables 0 - 180 degree servo rotation at 2 microseconds per step.
- Serial Command Format - The PSC supports several commands that are sent to it via RS-232 serial protocol. The voltage swing of this serial line is 0-5 VDC (TTL level). Each serial command must be preceded with an exclamation point, "!", and the pair of letters, "SC". This allows different types of AppMods to use the same serial line as the PSC.

3.3.2 Dynamixel CM-2+ Robot Controller

Dynamixel CM-2+ Control Module is a central control device that controls the servos of Dynamixel series (Figure 3.9). With this device, that can be operate the dynamixel motors and read information from the sensor. It also allows to construct and program joint type robots. The CM-2+ Control Module supports RS-485 and TTL communication and interlinks with all Dynamixel DX-series, RX-series and Sensor Module (AX-S1). A complete robot can be edited through the Motion Editor and Behavior Control Program. It is also supported by C language. The interface connects with ZIG-100 (wireless network module). (http://www.robotshop.ca/robotis-bioloid-cm-2control-module-3.html, 2010)

Figure 3.9 Dynamixel CM-2+ robot controller.

Dynamixel CM-2+ Control Module features:

(http://www.trossenrobotics.com/dynamixel-CM-2-plus-robot-controller.aspx, 2010)

- CPU : Atmega-128(128Kbyte Flash memory)
- Fuse for excess current interception

- Operating voltage : 7~18 V * Interface
- Dynamixel (AX-series) connector
- Dynamixel (DX-series, RX-series) connector
- ZIG-100 (wireless communication module) connection possibility
- LED : TX, RX, AUX
- RS-232C Serial Port (PC connection)
- 6 Buttons (5 input + reset button) : compatible with CM-5 * Operation method
- Boot loader (binary or Hex file download and play function)
- PLAY mode being compatible with Bioloid behavior control program
- Dynamixel management mode (MANAGE mode) - Motion editing mode (PROGRAM mode)

3.4 Sensors

A sensor is a device which generates an electrical signal when there is a physical action. In robotics, there are many physical sizes need to be measured. Angles, toques, velocities, accelerations and reaction forces are some of them. Bided robot AHTO has only an accelerometer sensor. On the other hand, RUBI's actuators' sensors give positions, toques, speeds, temperatures and voltages feedback. Also it has an accelerometer sensor. The information coming from an accelerometer can be divided into two parts; instantaneous accelerations and tilt values. In this work, only tilt values are used to determine robot's state which is walking balanced and unbalanced.

For this purpose, accelerometer data, which is filtered by low pass filter, is used to get disturbance direction. After determining the disturbance direction and strength, the robot can manipulate itself by applying several scenarios with related joints motors. If the disturbance strength is too high, the robot can step up or down to overcome disturbance. So, robot tries to overcome physical disturbances by using acceleration data. In this application, only the disturbances at the sagittal plane are interested.

3.4.1 Hitachi H48C 3-Axis Accelerometer Module

The Hitachi H48C 3-Axis Accelerometer is an integrated module that can sense gravitational (g) force of ±3g on three axes (X, Y, and Z). The module contains an onboard regulator to provide 3.3-volt power to the H48C, analog signal conditioning, and an MCP3204 (four channel, 12-bit) analog-to- digital converter to read the H48C voltage outputs. All components are mounted on a breadboard-friendly, 0.7 by 0.8 inch module. Acquiring measurements from the module is simplified through a synchronous serial interface.

Figure 3.10 Hitachi H48C 3-Axis Accelerometer.

Hitachi H48C 3-Axis Accelerometer features:

(http://www.parallax.com/Store/Microcontrollers/BASICStampModules/tabid/134/ProductID/97, 2010)

- Measure ±3 g on any axis.
- Uses MEMS (Micro Electro-Mechanical System) technology, with compensation for calibration-free operation.
- Onboard regulator and high-resolution ADC for simple connection to microcontroller host - compatible with BASIC Stamp 2 series SHIFTOUT and SHIFTIN commands.
- Free-fall output indicates simultaneous 0g an all axes.
- Small package: 17.8 mm x 20.3 mm. Wide operational range: -25° to 75° C

CHAPTER FOUR
WALKING PATTERN GENERATION

To find the required actuator characteristics, it is necessary to formulate and solve the equations of the kinematics and dynamics of the biped robot mechanisms. Many researchers use different simulation programs and mathematics models to solve this problem (Huang et al., 2000, 2001, Ha et al., 2007). In this thesis, CosmosMotion that is the part of SolidWorks is used a simulation program. By using this program, the robot motion can be simulated and the necessary joint actuators torques, projection angles, angular and linear velocities, angular and linear accelerations and the reaction forces can be calculated.

The necessary constrains and equations to generate walking pattern of the biped robot are discussed in the chapter two. Depends on these equations and with the design parameters, AHTO motion was simulated on CosmosMotion.

In the chapter two, it is mentioned that using third-order interpolation is best way to find walking trajectories. It is seen that cubic polynomial and cubic spline interpolation are useful methods, when looking at the mathematical background. Thant & Aye (2009) studies bring out that the cubic spline interpolation curve is smoother than the cubic polynomial curve. Therefore, it is the best method for trajectory planning and cubic spline interpolation was used in this thesis.

The physical parameters of the biped robot AHTO are shown in Table 4.1.

Table 4.1 The physical parameters of the AHTO.

Length (cm)	l_{tr}	l_{th}	l_{sh}	l_{an}	l_{ab}	l_{af}	
	11,55	7,7	7,46	7,5	4,48	6,53	
Mass (gram)	m_0	m_1	m_2	m_3	m_4	m_5	m_6
	160	80	80	48	48	45	45

4.1 Foot and Hip Trajectories

Walking trajectory generation is a complex problem. To solve these complex kinematic and dynamic problems, there are many assumptions in the literature (Nagasaka et al., 1999, Hong, 2009 & Huang et al., 2001). These assumptions become easier the solutions of the complex problem.

Simulating AHTO's simple one step, it was assumed that the foot move was parallel to the ground ($\theta_a \ t$ =0), the ground surface was flat ($q_{gs}(k) = q_{ge}(k) = 0$, $h_{gs}(k) = h_{ge}(k) = 0$), the step length was 9 cm/step with the step period of 0,9 s/step and the position and time of the highest point of the swing foot ankle were L_{ao} = 10 cm, H_{ao} = 10 cm, T_m = 0,5 s and T_d = 0,15 s.

With these parameters, foot and hip trajectory were achieved by using MATLAB.

Figure 4.1 shows the foot trajectory along x-axis according to equation (2).

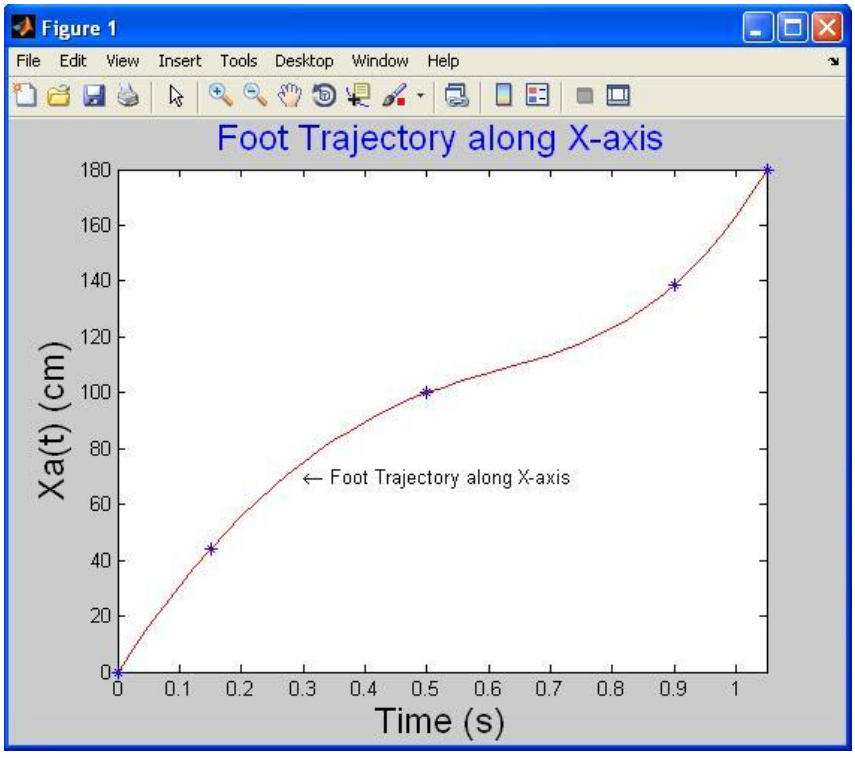

Figure 4.1 Foot trajectory along x-axis.

Figure 4.2 shows the foot trajectory along z-axis according to equation (3).

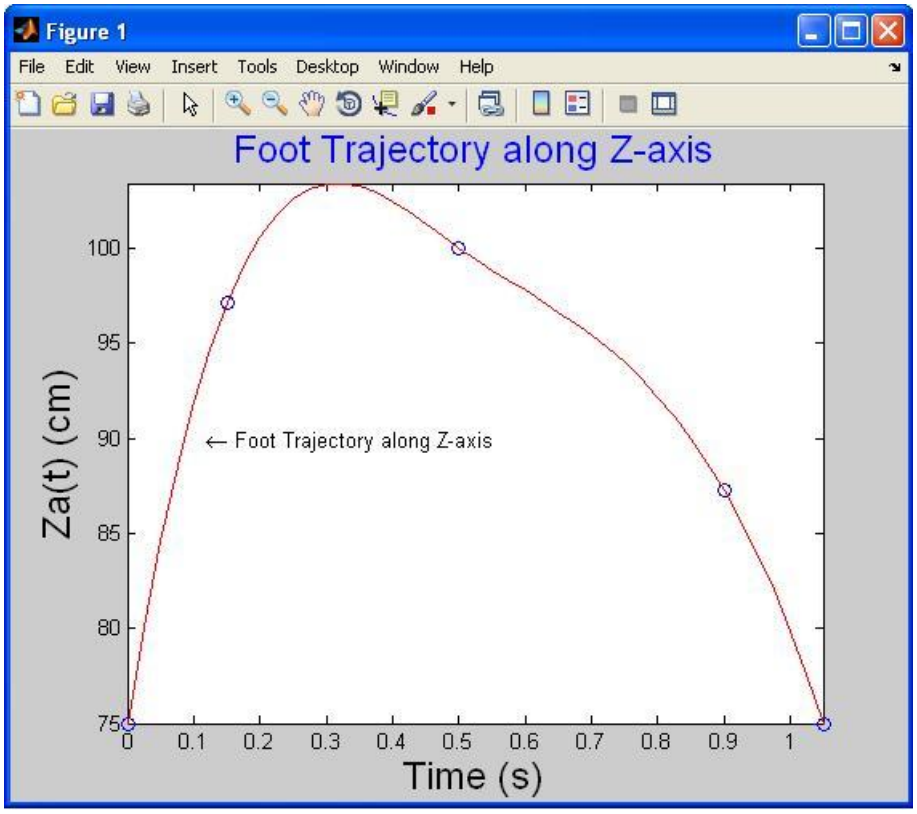

Figure 4.2 Foot trajectory along z-axis.

Obtaining data $x_a\ t$ and $z_a\ t$ were entered the CosmosMotion's move and achieved the foot trajectory (Figure 4.3).

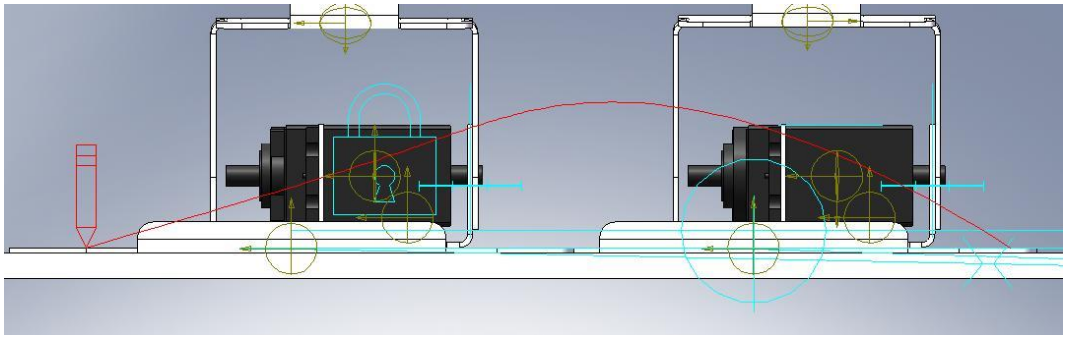

Figure 4.3 Foot trajectory.

At the hip motion, it was assumed that the biped robot hip moved between $H_{h\min}$ = 320 cm and $H_{h\max}$ =330 cm. Also, distances along to x axis from the hip to the ankle of the support foot at the start x_{sd} = 38 cm and distances along to x axis from the hip to the ankle of the support foot at the end x_{ed} = 38 cm.

Figure 4.4 shows the hip trajectory along x-axis according to equation (5).

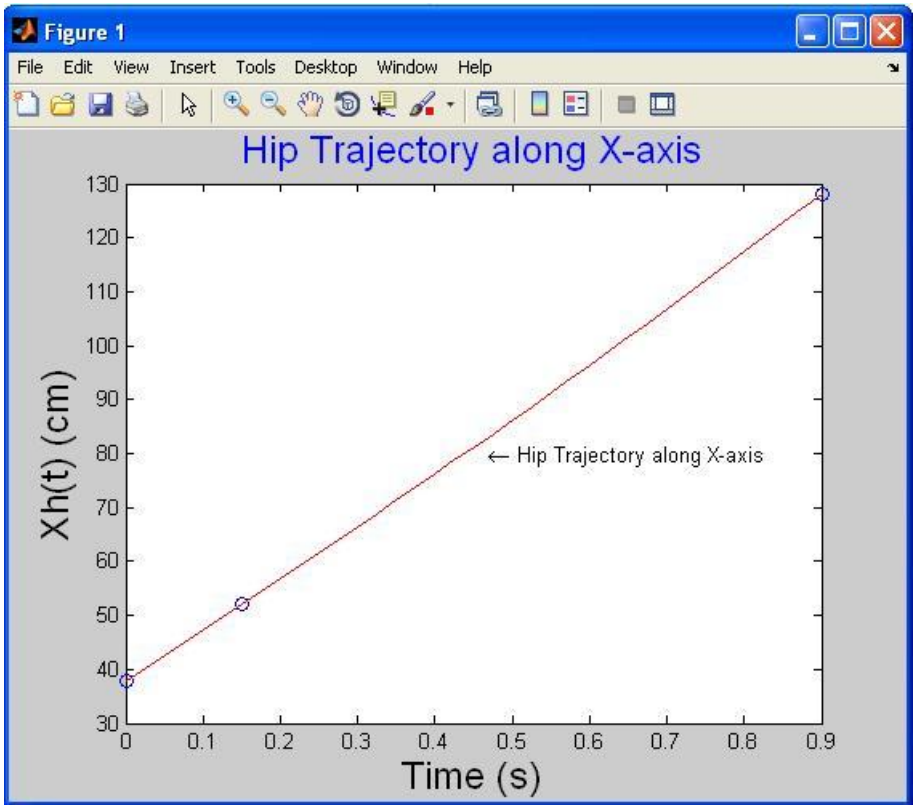

Figure 4.4 Hip trajectory along x-axis.

Figure 4.5 shows the hip trajectory along z-axis according to equation (4).

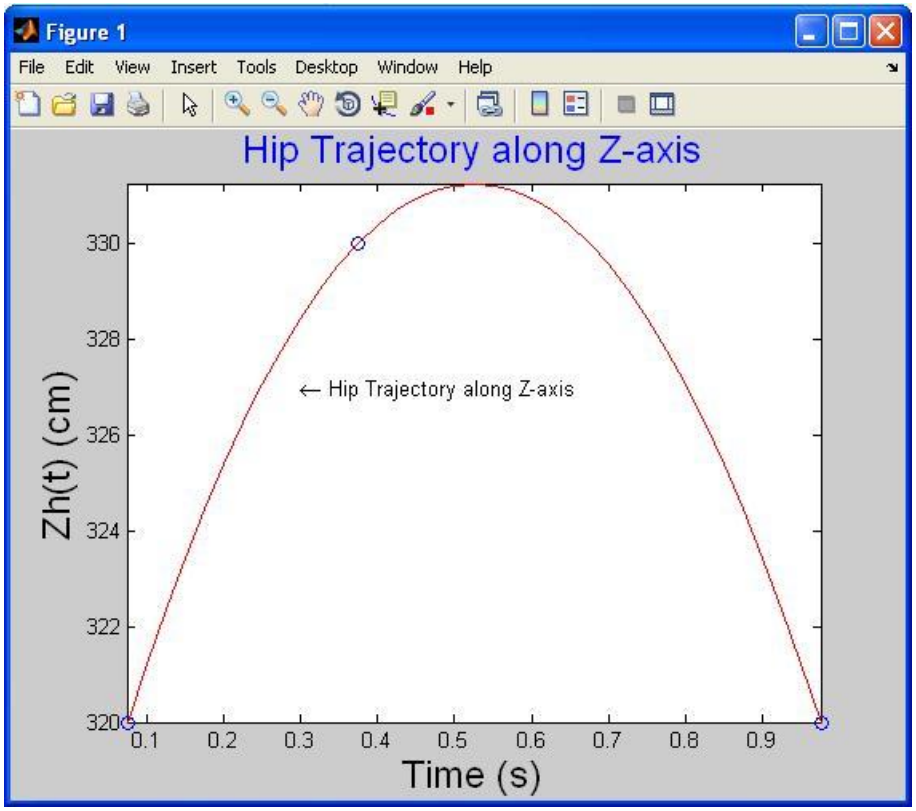

Figure 4.5 Hip trajectory along z-axis.

Obtaining data $x_h\ t$ and $z_h\ t$ were entered the CosmosMotion's move and achieved the hip trajectory (Figure 4.6).

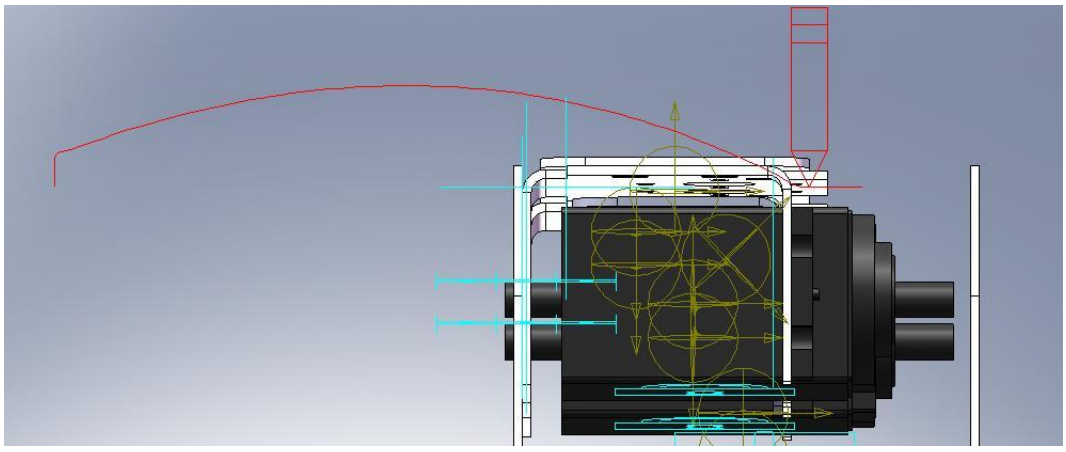

Figure 4.6 Hip trajectory.

The foot trajectory and hip trajectory were used for the inverse kinematics that is an answers the question, “given the desired position of the robot’s body parts, what must be the angles at all of the robot’s joints?” Figure 4.7 and 4.8 are snapshots of inverse kinematics simulation.

Figure 4.7 Simulation view of biped robot at the sagittal plane.

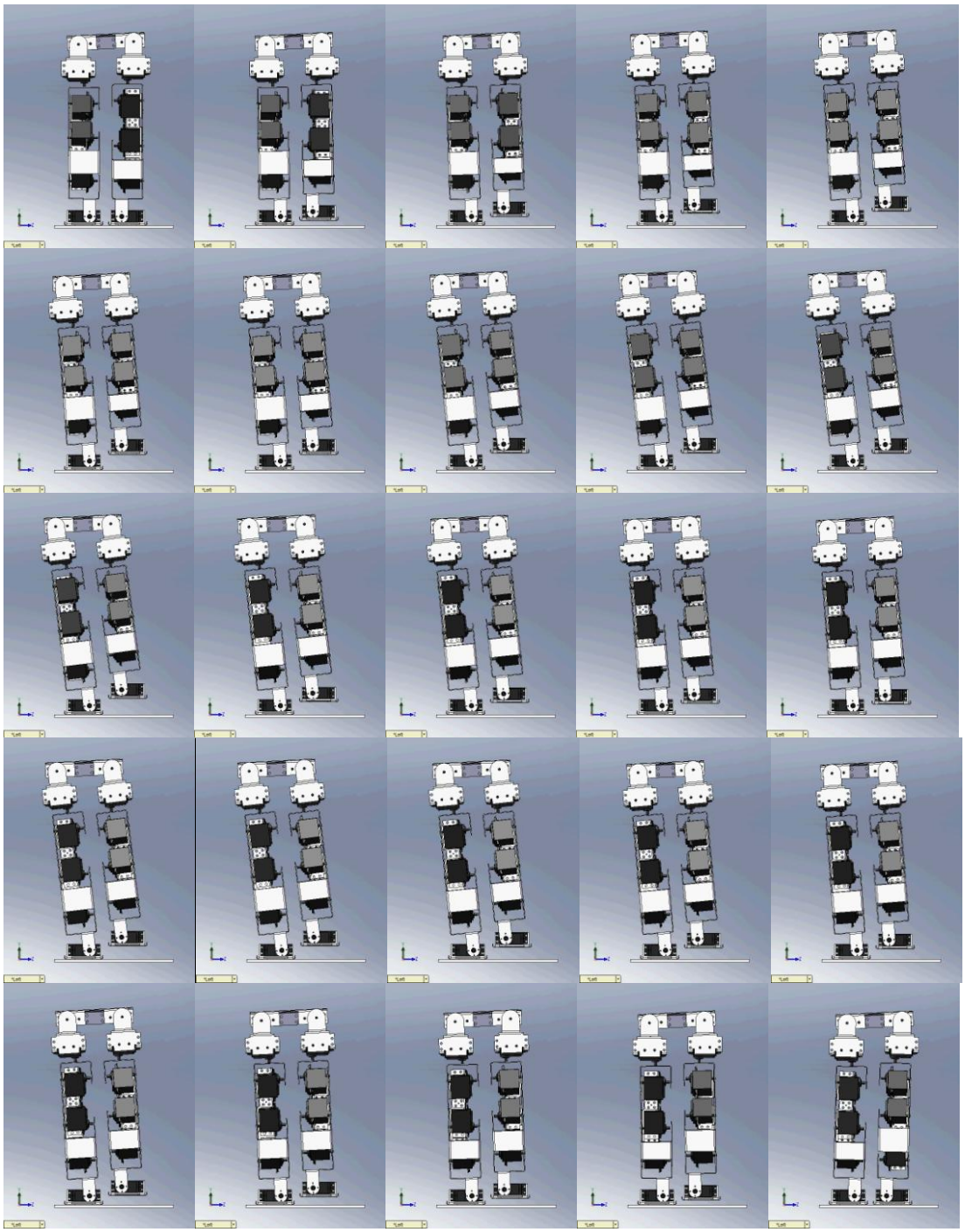

Figure 4.8 Simulation view of biped robot at the frontal plane.

Although, this work only interested in walking at the sagittal plane, moving on the frontal plane was used to become easy the simulation. At the frontal plane, only hip moving was considered. An assumption at the frontal plane, hip trajectory along y-axis is created by spline curve, shown in Figure 4.9.

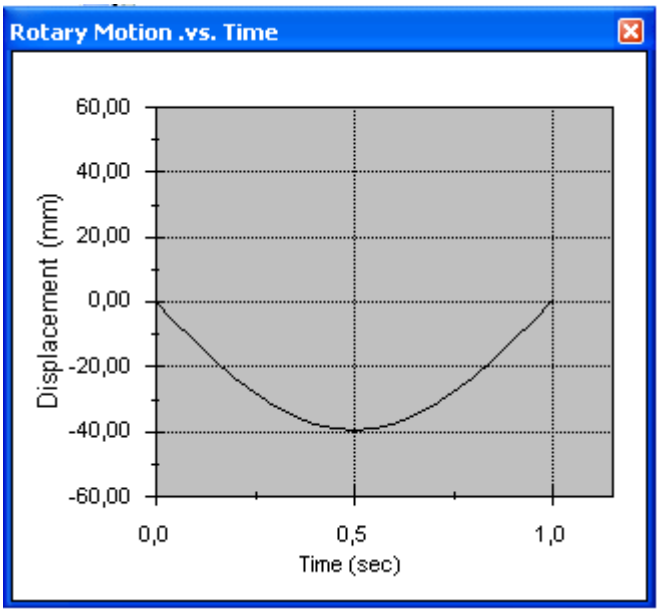

Figure 4.9 Hip trajectory along y-axis at the frontal plane.

4.2 Joints Angles

After finishing the simulation, all joint angles were achieved in joint properties. Joint angles are important data at the simulation. They are used as an input data for joint actuators and forward kinematics simulation.

All joints angles changes of AHTO shown in Figure 4.10. When looking up the joints angles at the sagittal plane (Figure 4.10. a,b,e,f,g,h), it is seen that the angles changed maximum 50 degrees. At the one simple step, ankle joints angles changed between 0 to -33 and -13 to 31 degrees, knee joints angels changed between -2 to 31 and 0 to 50 degrees and hip joints angles changed between 0 to 48 and 0 to -43 degrees.

With assumptions, the joints angles at other planes moved in small value and changed maximum 8 degrees. (Figure 4.10. c,d,i,j,k,l).

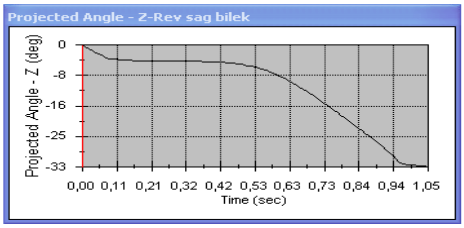

a) Right ankle joint angles changes.

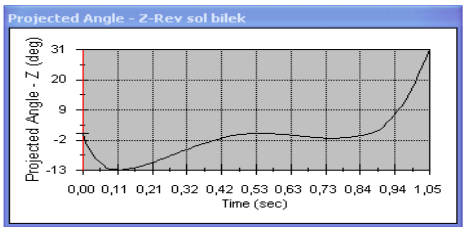

b) Left ankle joint angles changes.

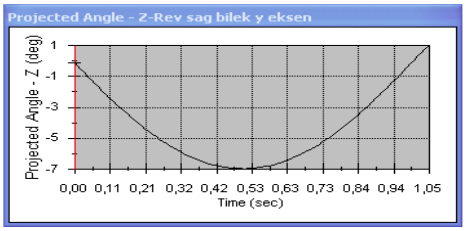

c) Right ankle joint angles in x-axis changes.

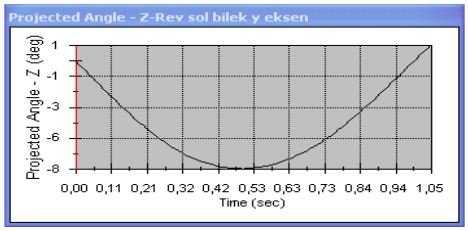

d) Left ankle joint angles in x-axis changes.

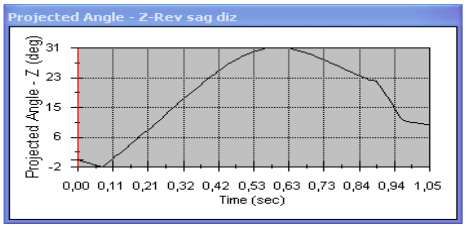

e) Right knee joint angles changes.

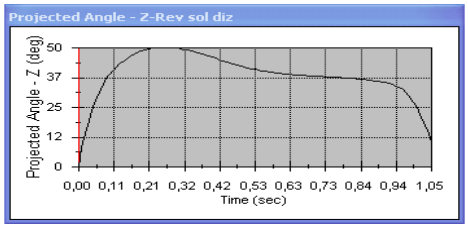

f) Left knee joint angles changes.

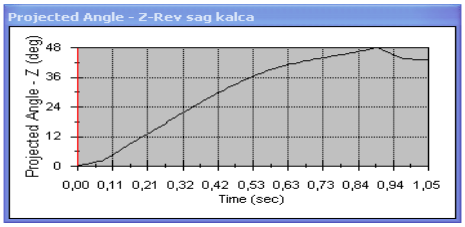

g) Right hip joint angles changes.

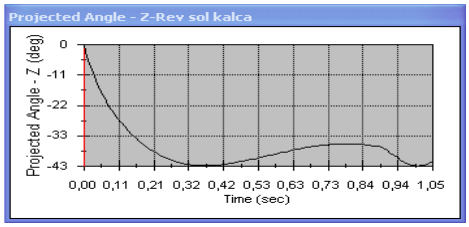

h) Left hip joint angles changes.

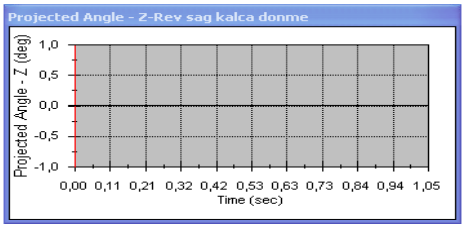

i) Right hip joint angles in z-axis changes

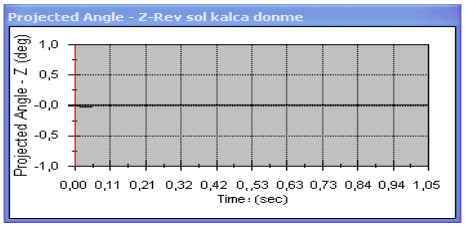

j) Left hip joint angles in z-axis changes.

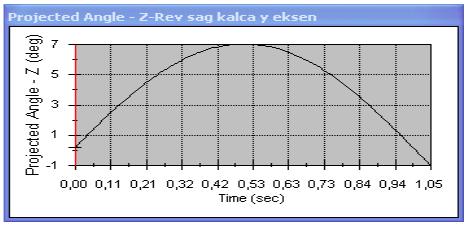

k) Right hip joint angles in x-axis changes.

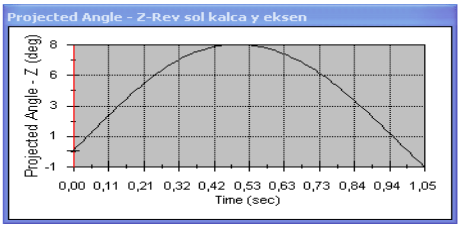

l) Left hip joint angles in x-axis changes.

Figure 4.10 Joints angles of biped robot AHTO for one single step

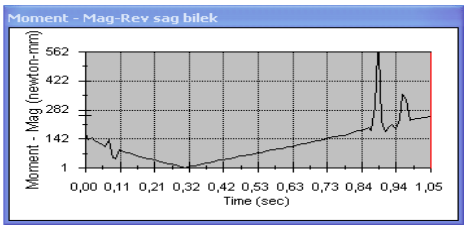

a) Right ankle joint torques changes.

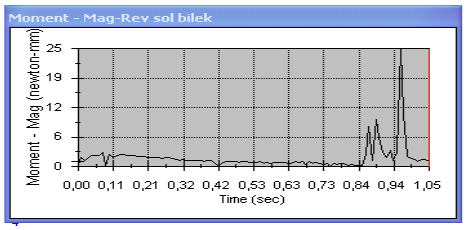

b) Left ankle joint torques changes.

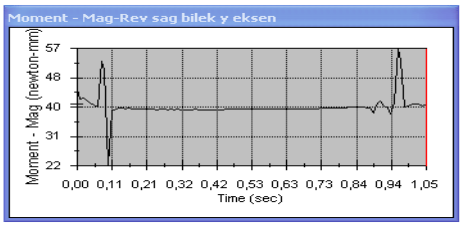

c) Right ankle joint torques in x-axis changes.

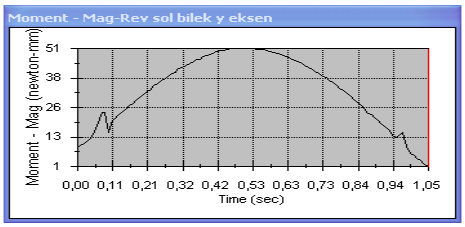

d) Left ankle joint torques in x-axis changes.

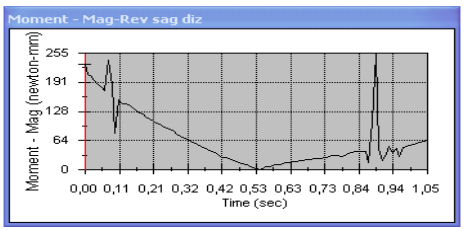

e) Right knee joint torques changes.

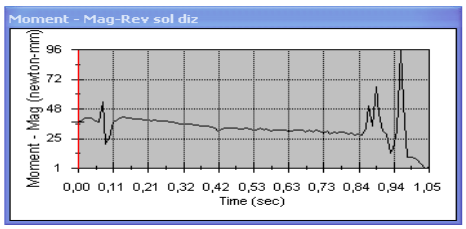

f) Left knee joint torques changes.

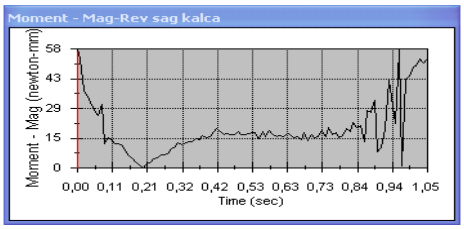

g) Right hip joint torques changes.

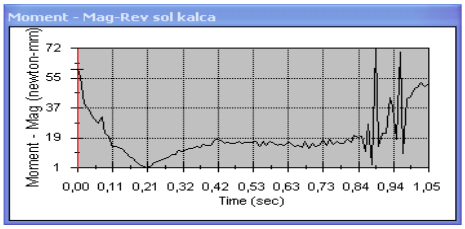

h) Left hip joint torques changes.

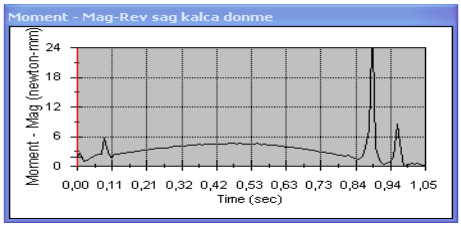

i) Right hip joint torques in z-axis changes

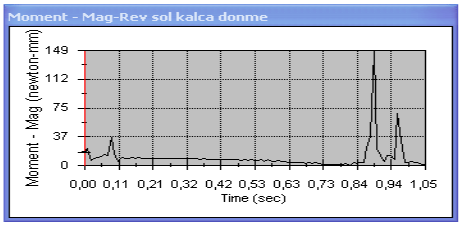

j) Left hip joint torques in z-axis changes.

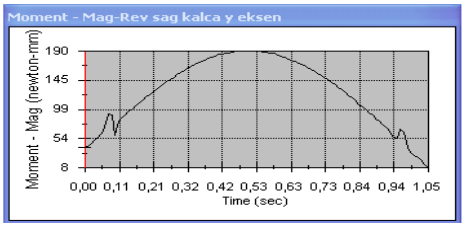

k) Right hip joint torques in x-axis changes.

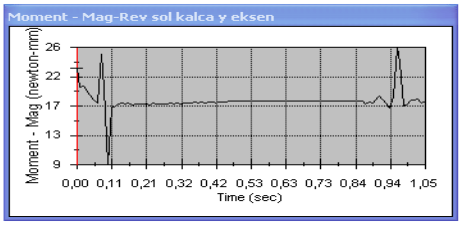

l) Left hip joint torques in x-axis changes.

Figure 4.11 Joints torques of biped robot AHTO for one single step

4.3 Joints Torques

To reach joint torques, joints angles which are obtained from inverse kinematics, are given as an input data to joints properties in CosmosMotion. This is known as the forward kinematics, which is the answer, "given the angles at all of the robot's joints, what are the positions of the robot's parts?" in robotics. After the forward kinematics, all important data like torques, velocities, accelerations, forces can be obtained from simulation.

All joints torques changes of AHTO shown in Figure 4.11. When looking up the results at the sagittal plane (Figure 4.11. a,b,e,f,g,h), it is seen that the maximum torque was 562 N.mm (5,73 kg.cm) at the support foot ankle joint. Maksimum torque at left ankle joints torque was 25 N.mm, at right knee joints was 57 N.mm, at left knee joints was 96 N.mm, at right hip joints 58 N.mm and at left hip joints 72 N.mm.

Maximum joint torque at other planes was 255 N.mm at right ankle joint in x-axis. (Figure 4.11. c,d,i,j,k,l).

The ZPM trajectory in Figure 4.12 is near the center of stable region. Thus, the robot has a large stability margin.

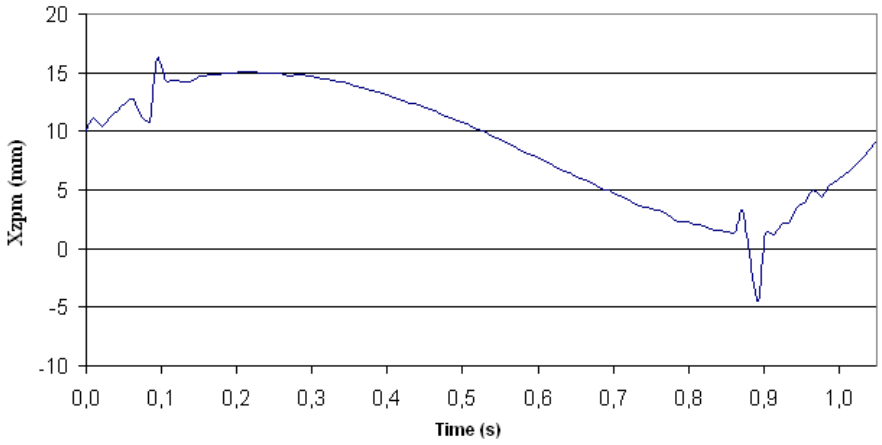

Figure 4.12 ZPM trajectory in the hip coordinate system

Biped robot AHTO was used to test the results of proposed method and simulation. AHTO's properties were given in Chapter 2. Experiment was done with parameters to be computed at Chapter 3. Figure 4.13 is a snapshot of walking experiment.

Figure 4.13 Walking experiments snapshots.

CHAPTER FIVE
CONCULUSIONS AND FUTURE WORKS

In this thesis, the main objective was to develop and realize a biped robot mechanism. For this purpose, the biped robot AHTO and RUBI were developed according to our design philosophy. The robots designed with all of mechanical structure, hardware devices, motor controllers and sensors devices. It was aimed that biped mechanisms could be more effective in term of walking gait and energy consumption. For that purpose, two main studies were worked out:

- Mechanical design
- Walking trajectories generation and to obtain robot's joint properties during the walking phase.

In mechanical design phase, two different biped robot designs were applied. The first design AHTO was built with a standard servo and its mechanical structure depend on this servo. Due to the disadvantages of the first robot, the second one, which is more human-like, was designed.

Our last mechanical model RUBI is based on human shape and 1/ 2.3 ratios in all leg dimensions. The motor placements and joint movements are figured as much as similar to human leg structure.

In the walking phase, for one single step period, foot and hip trajectories, joints angles, velocities, accelerations and torques were calculated by using computer simulations. The dynamic balance in walking trajectory was achieved the point on the ground about which the sum of all the moments of the active forces equal zero by using the zero moment point (ZPM) criteria.

It was investigated not only the theoretical calculations and computerized simulations, but also experiments on robot mechanism in the walking analysis phase. At the same time, robot mechanical structure was realized. Robots motors and

control circuits were obtained, and then, one step walking trajectory was applied to model robot.

Of course the more realistic walking gait applications and more complex control algorithm is required to final work. But this study is responsible for only mechanical design and walking trajectory extraction.

With this work, it is concluded that:

- Due to mechanical design of biped robot, one must be aware of human-like gait fundamentals, walking robot structures are very complex in order to design.
- The mechanical structure must be as strong as to weight to all robot parts including case, motors, sensors, controllers an also batteries.
- Some joints like ankles are important in design, because those joints must be strong for all loads and the momentum in some walking instants.
- In this thesis, walking trajectory calculations are based on ZMP method. ZPM only one axis is used. But in real life problem all axes must be considered by using other criteria and methods in the future studies. .
- Robot balance which is based on ZMP method would be supported by other feedback facilities. In our study, all smart robot motors in second design can return position load temperature voltage information in order to use in complex control algorithms. That option will help in the future studies.
- Additionally our robots are equipped with accelerometer which can supply accelerations and tilt angles in three axes. That equipment is placed at trunk point which can be near the center of mass. This option may increase the success of balance algorithm. Due to the fast respond to external effects which can deform the walking sequence.
- Parallel with this study, complex control applications are being investigated. Two main works are currently in progress: First one is about computer-aided control system which is based PID control block on simulink, and the second study is based on embedded ARM microcontroller for stand-alone robot

applications. In the future, with the end of one of those studies, more controllable and efficient walking robot system may be achieved.

- In the future, more realistic full body humanoid robot structures may be developed in our laboratory in the light of this study and the hand on experience. Those robotic structures need dynamic and static mechanical analysis and more sophisticated electronic circuits and control algorithms. For this purpose, PhD and master subjects can be evaluated.

REFERENCES

Chevallereau C., Bessonnet G., Abba G. & Aoustin Y.(Eds). (2009). *Bipedal robots: modeling, design and walking synthesis.* Great Britain, Wiltshire: Iste &Wiley.

Dasgupda, A., & Nakamura. Y. (1999). Making feasible walking motion of humanoid robots from human motion capture data. *Proceedings IEEE International Conference on Robotics and Automation, 14* (4), 1044-1049.

Dynamixel CM-2+ Robot Controller. (n.d.). Retrieved May 16, 2010, from http://www.trossenrobotics.com/dynamixel-CM-2-plus-robot-controller.aspx.

Ha, S., Han, Y., & Hahn, H. (2007). Adaptive gait pattern generation of biped robot based on human's gait pattern analysis. *International Journal of Mechanical Systems Science and Engineering*, *1* (2).

Hirai, K., Hirose, M., Haikawa, Y & Takenaka, T. (1998). The development of Honda humanoid robot. *Proceedings of the 1998 IEEE International Conference on Robotics & Automation*, 1321-1326

Hitachi H48C 3-Axis Accelerometer. (n.d.). Retrieved May 16, 2010, from http://www.parallax.com/Store/Microcontrollers/BASICStampModules/tabid/134/ProductID/97.

Huang, Q., Nakamura, Y., Arai, H., Tanie, K., (2000). Development of a biped humanoid simulator. *Proc. Int. Conf. Intelligent Robot and Systems*, 280-289.

Huang, Q., Yokoi, K., Kajita, S., Kaneko, K., Arai, H., Koyachi, N., et al. (2001). Planning walking patterns for a biped robot. *IEEE Transactions on Robotics and Automation*, *17* (3), 280-289.

Hong, S., Oh, Y., You, B. & Oh, S. (2009). A walking pattern generation method of humanoid robot MAHRU-R. *Intelligent Service Robotics journal*, *2*(3), 161-171

Inman, V.T., Ralston, H.J., & Todd, F. (1981). *Human walking*. Baltimore, MD: Willams & Wilkins.

Ito, D., Murakami, T. & Ohnishi, K. (2002). An approach to generation of smooth walking pattern for biped robot. *Proceedings of the 7th Workshop on Advance Motion Control Malibor, Slovenia*, 98-103

Kim, J. H. & Oh, J. H. (2004). Realization of dynamic walking for the humanoid robot platform KHR-1. *Advanced Robotics journal*, *18*(7), 749-768

Li, Q., Takaniski, A. & Kato, I. (1992). Learning Control of Compensative Trunk Motion For Biped Walking Robot Based On ZMP Stability Criterion. *Proceedings of the 1992 IEEE/RSJ International Conference on Intelligent Robotics & Systems*, 597-603

McMahon, T. A. (1984). *Muscles, reflexes, and locomotion*. Princeton, NY: Princeton University Press.

Murphy, K. N. & Raibert, M. H. (1985). Trotting and bounding in a planar two-legged model. *In 5th Symposium on Theory and Practice of Robots and Manipulators*, 411-420

Nagasaka, K., ınoue, H. & Inaba, M.(1999). Dynamic Walking Pattern Generation for a Humanoid Robot Based on Optimal Gradient Method. *Proceedings of the 1999 IEEE International Conference on Systems, Man & Cybernetics*, *6*, 908-913

Parallax Servo Controller. (n.d.). Retrieved May 16, 2010, from http://www.parallax.com/Store/Accessories/MotorServoControllers/tabid/160/ProductID/376/

Park, J. H. & Kim, K. D. (1998). Biped Robot Walking Using Gravity-Compensated Inverted Pendulum Modeand Computed Torque Control. *Proceedings of the 1998 IEEE International Conference on Robotics & Automation,* 3528-3533

Raibert, M. H. & Sutherland, I. E. (1993). Machines that walk. *Scientific American, 248*(2), 44–53

Raibert, M. H. (1986). *Legged Robots that Balance*. Cambridge: MIT Press

Robotis Bioloid CM-2+ Control Modul. (n.d.). Retrieved May 16, 2010, from http://www.robotshop.ca/robotis-bioloid-cm-2control-module-3.html

Robotis Bioloid Dynamixel RX-28 Smart Serial Servo. (n.d.). Retrieved May 16, 2010, from http://www.robotshop.ca/robotis-cx-28-serial-servo-3.html

Shih, C. L. (1997). Gait synthesis for a biped robot. *Robotica journal*, *15*, 599-607

Tang, J., Zhao, Q., & Huang, J. (2007). Application of "human-in-the-loop" control to a biped walking-chair robot. *Systems, Man and Cybernetics, 2007. ISIC. IEEE International Conference,* 2431 – 2436.

Tang, Z., Zhou, C. & Sun, Z. (2003). Trajectory planning for smooth transition of biped robot. *Proceedings of the 2003 IEEE International Conference on Robotics & Automation,* 2455-2460

Thant, A. A.,& Aye, K. K. (2009). Application of cubic spline interpolation to walking patterns of biped robot. *Proceedings of Word Academy of Science, Engineering and Technology*, *38*, 42-34

Vigor VS-2 servos. (n.d.). Retrieved May 16, 2010, from http://www.servodatabase.com /servo/vigor/vs-2

Vukobratoviç, M.,& Borovac, B. (2004). Zero moment point – thirty five years of its life. *International Journal of Humanoid Robotics, 1*(1), 157-73

Yamaguchi, J., Takaniski, A. & Kato, I. (1993). Development of a biped walking robot compensating for three-axis moment by trunk motion. *Proceedings of the 1993 IEEE/RSJ International Conference on Intelligent Robotics & Systems,* 561-566

APPENDIX A

DRAWINGS OF THE WALKING ROBOT

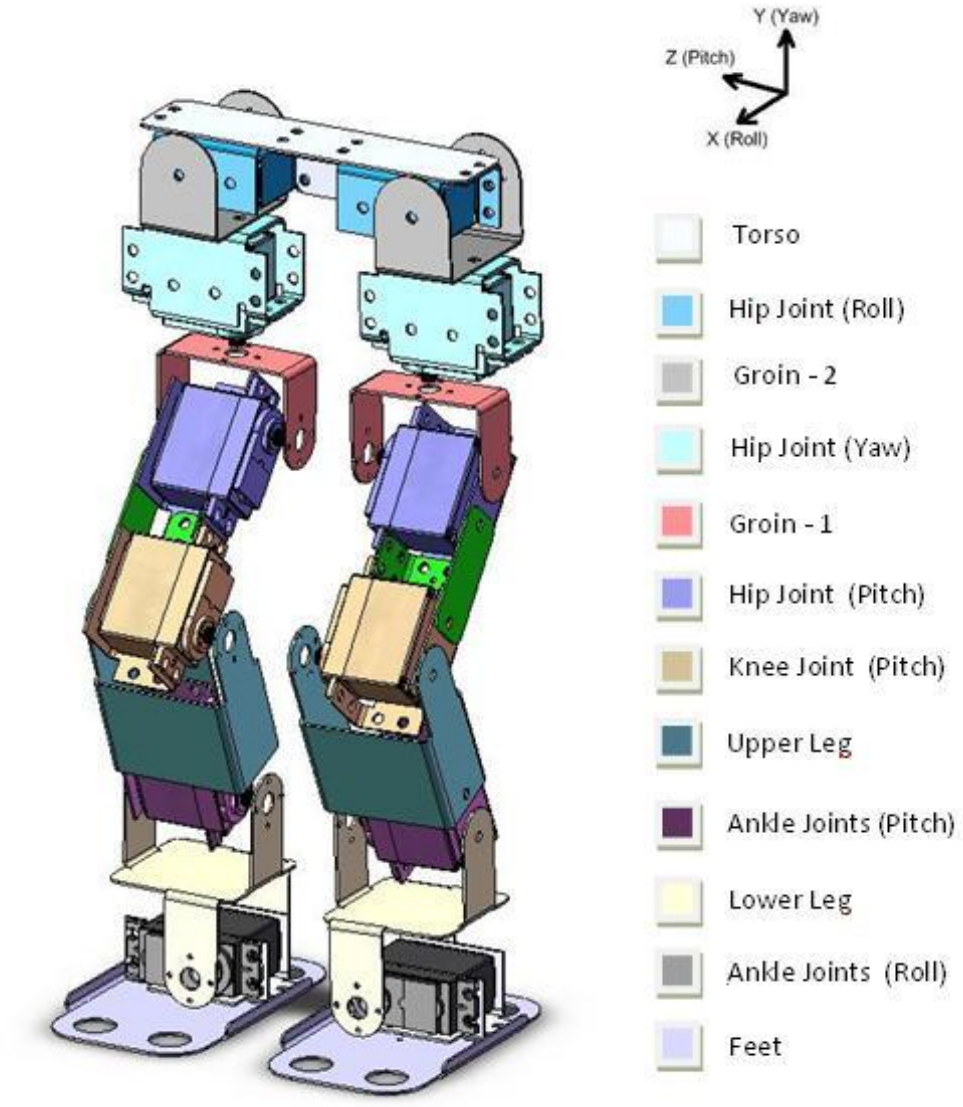

Figure 1 Parts of the biped walking robot AHTO.

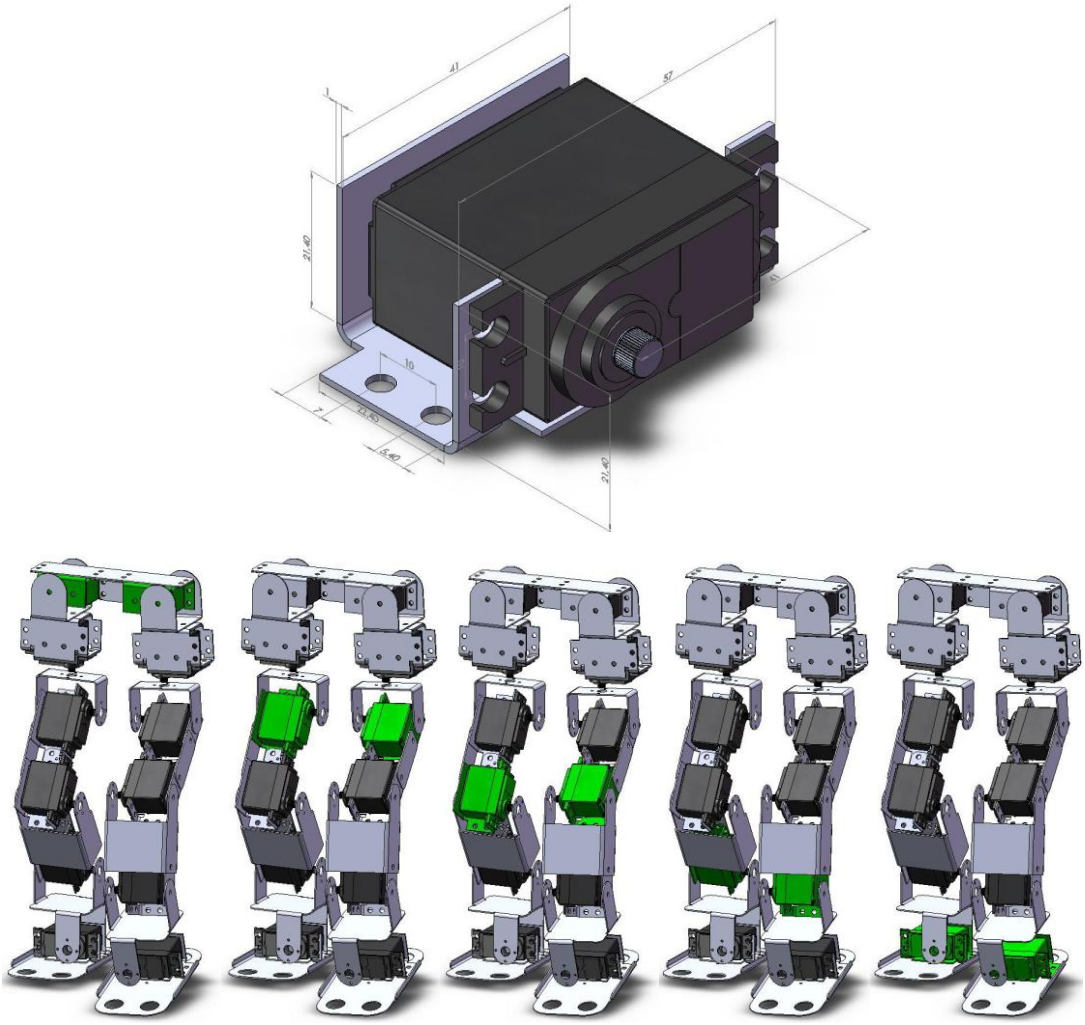

Figure 2 3D drawings of motors with servomotor bracket of hip joint (roll, pitch), knee joint, and ankle joint (pitch, roll).

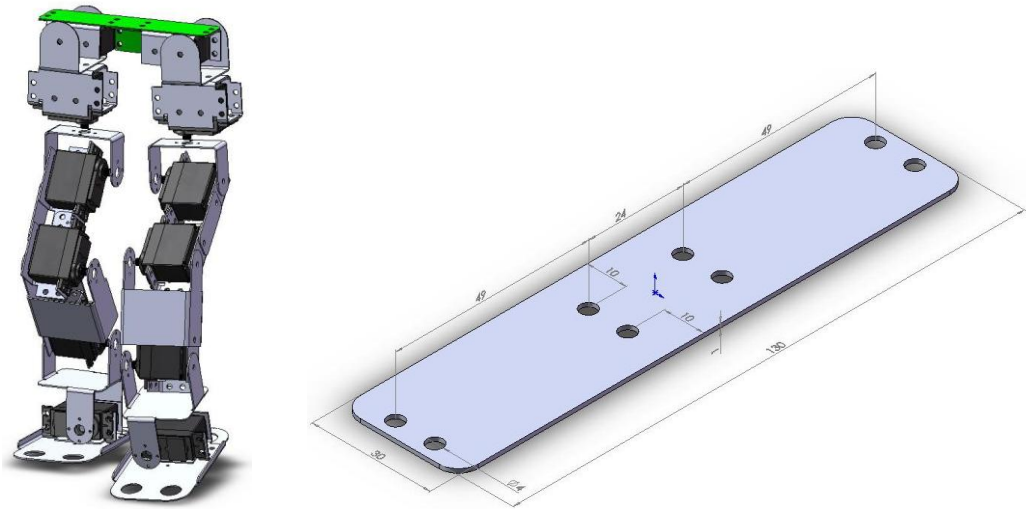

Figure 3 3D drawings of torso.

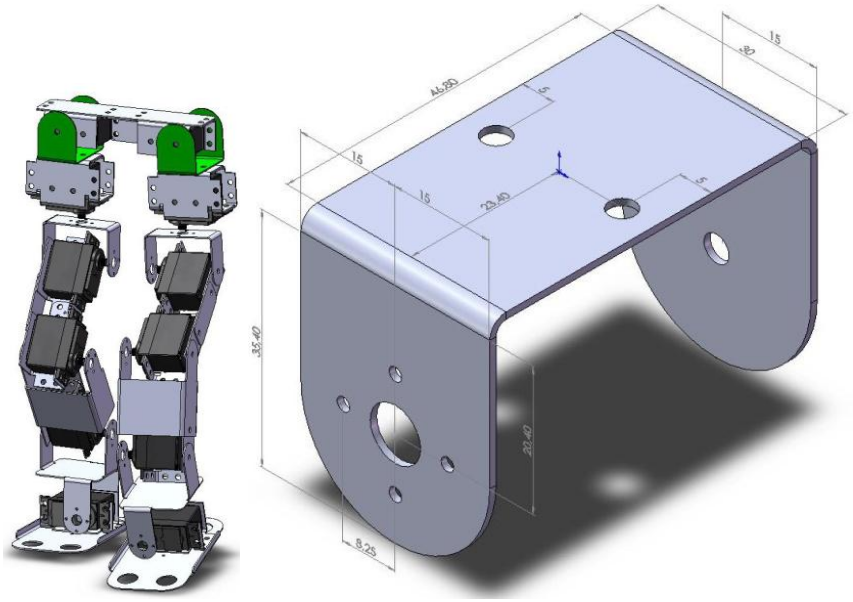

Figure 4 3D drawings of groin.

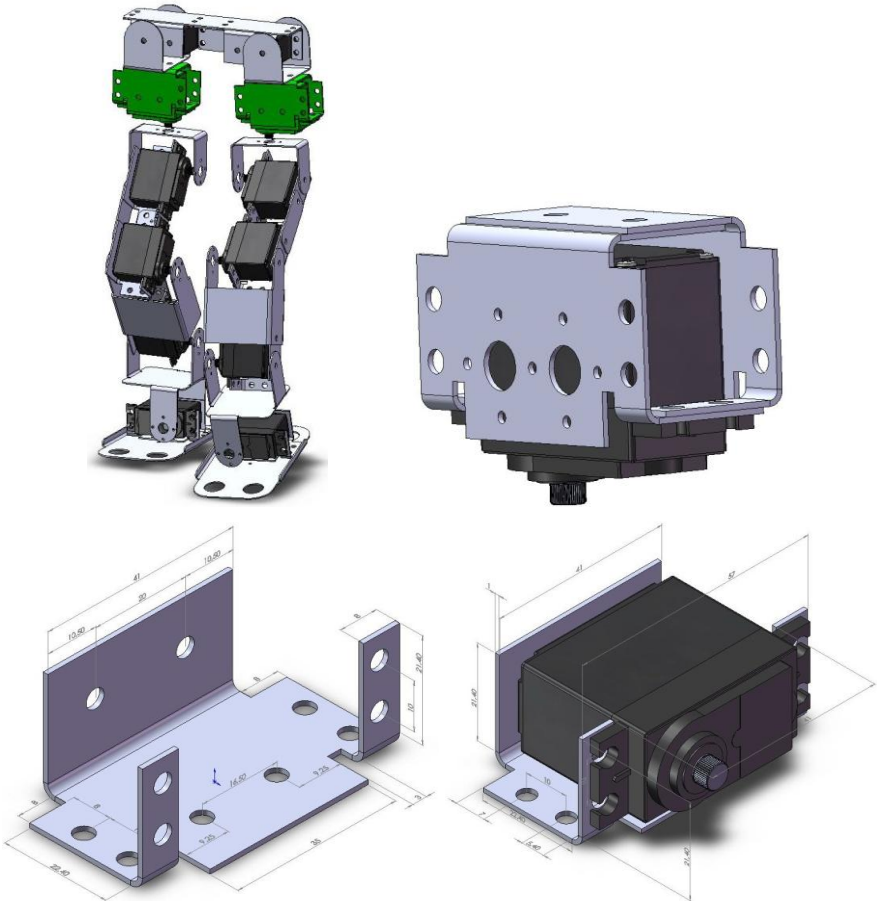

Figure 5 3D drawings of hip joint (yaw).

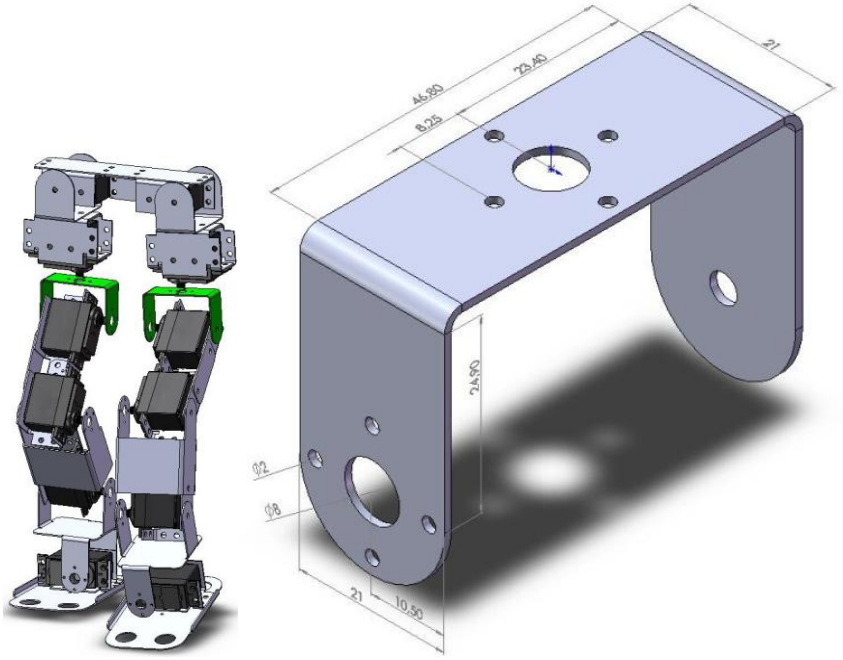

Figure 6 3D drawings of groin-1.

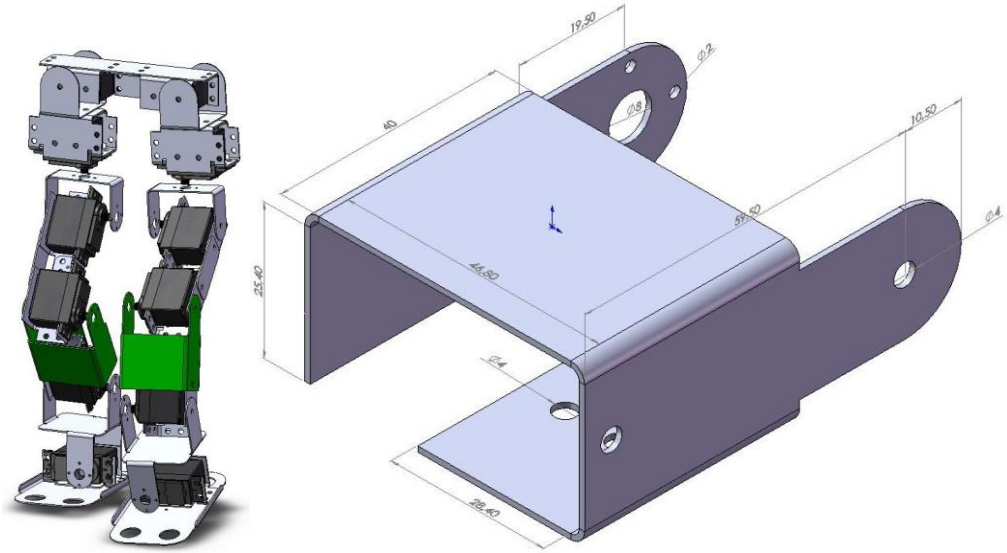

Figure 7 3D drawings of upper leg.

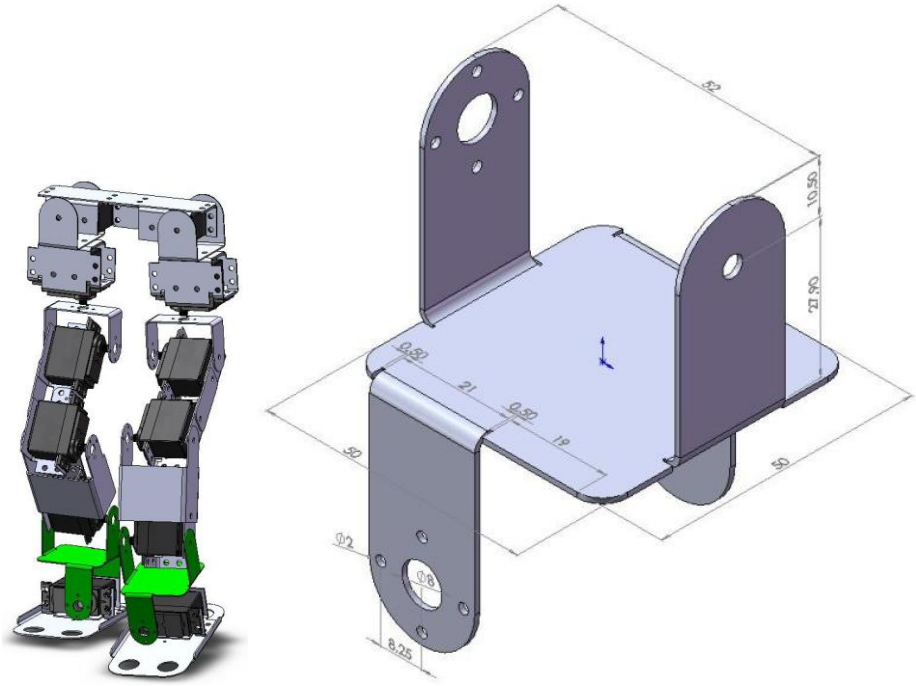

Figure 7 3D drawings of lower leg.

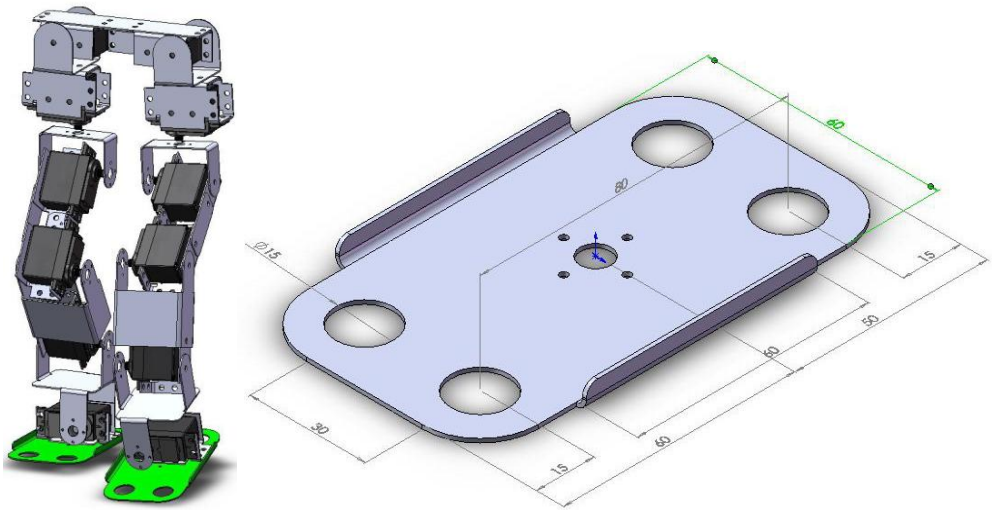

Figure 8 3D drawings of foot.

APPENDIX B

DRAWINGS OF THE WALKING ROBOT RUBİ

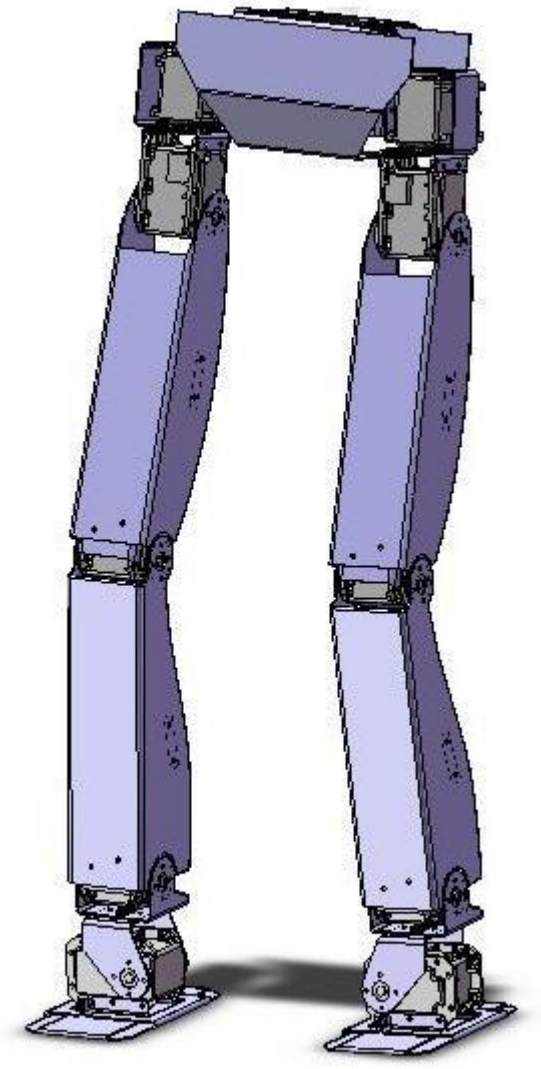

Figure 1 Parts of the biped walking robot RUBI.

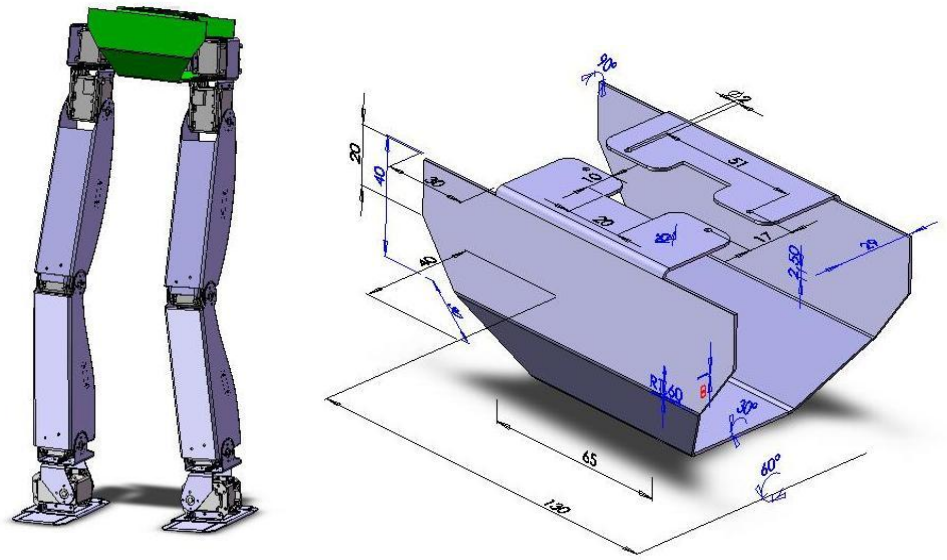

Figure 2 3D drawings of torso.

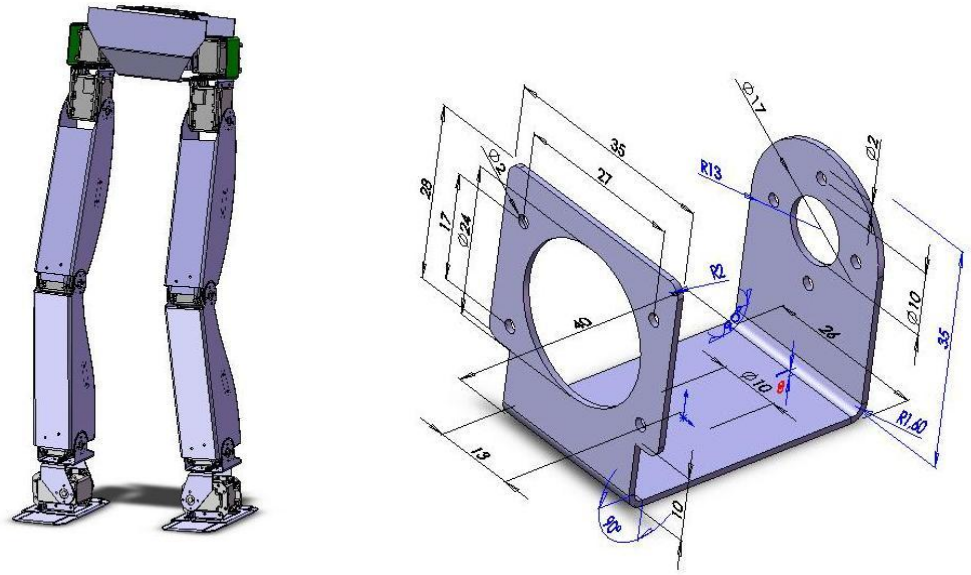

Figure 3 3D drawings of hip joint.

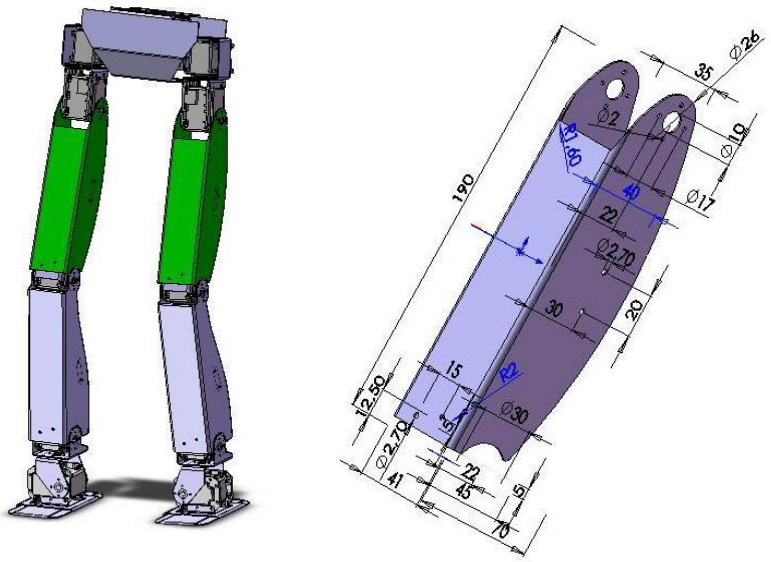

Figure 4 3D drawings of upper leg.

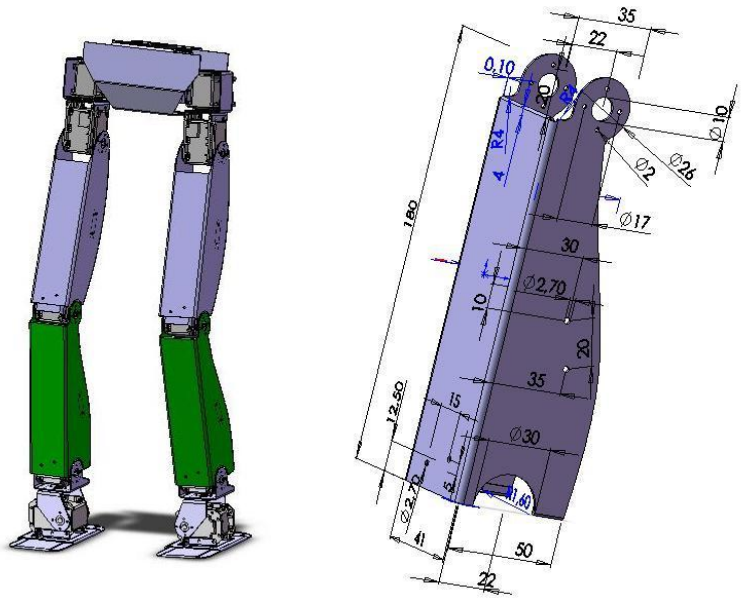

Figure 5 3D drawings of lower leg.

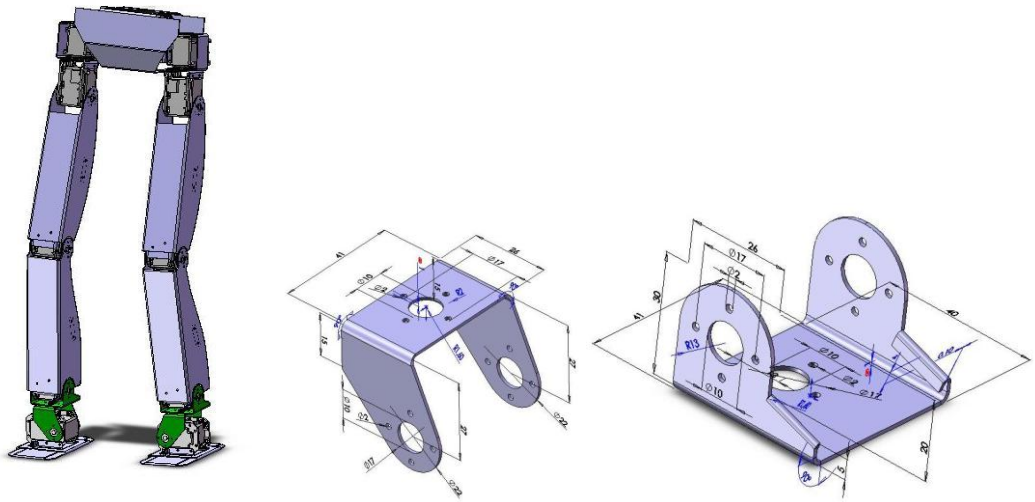

Figure 6 3D drawings of ankle.

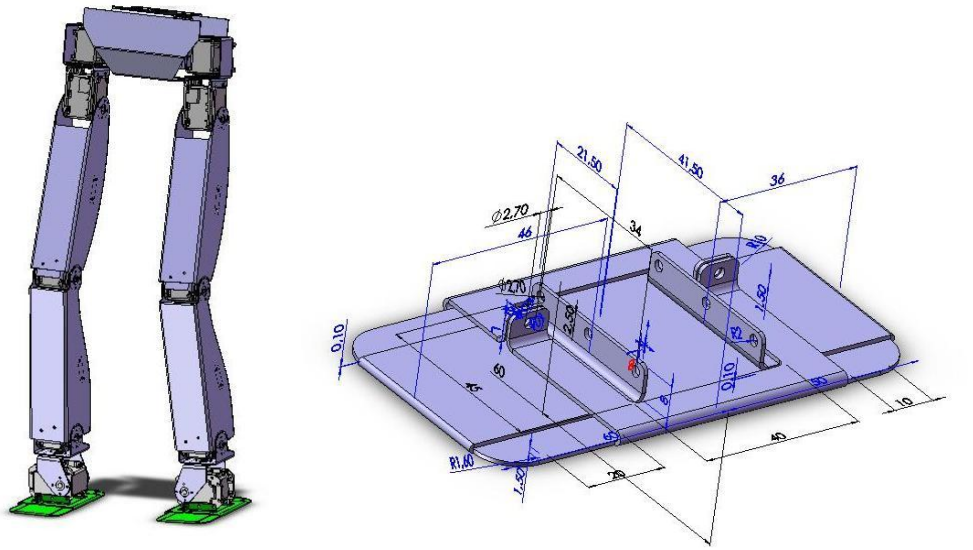

Figure 7 3D drawings of foot.

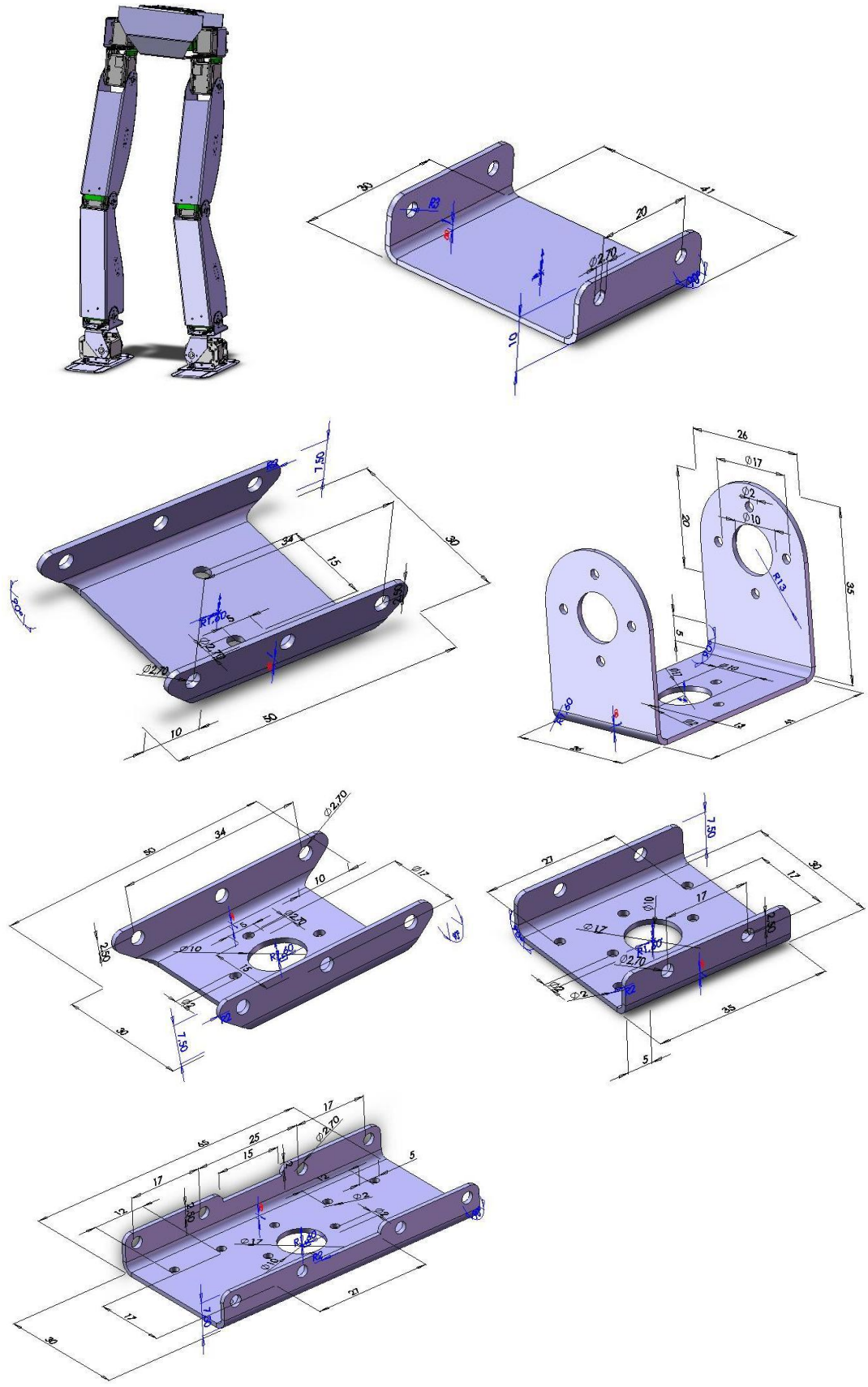

Figure 8 3D drawings of linkers.